EFDA–JET–PR(10)23

A. Loarte, V. Riccardo, J.R. Martin-Solís, J. Paley, A. Huber, M. Lehnen
and JET EFDA contributors

Magnetic Energy Flows during the Current Quench and Termination of Disruptions with Runaway Current Plateau Formation in JET and Implications for ITER

"This document is intended for publication in the open literature. It is made available on the understanding that it may not be further circulated and extracts or references may not be published prior to publication of the original when applicable, or without the consent of the Publications Officer, EFDA, Culham Science Centre, Abingdon, Oxon, OX14 3DB, UK."

"Enquiries about Copyright and reproduction should be addressed to the Publications Officer, EFDA, Culham Science Centre, Abingdon, Oxon, OX14 3DB, UK."

The contents of this preprint and all other JET EFDA Preprints and Conference Papers are available to view online free at www.iop.org/Jet. This site has full search facilities and e-mail alert options. The diagrams contained within the PDFs on this site are hyperlinked from the year 1996 onwards.

Magnetic Energy Flows during the Current Quench and Termination of Disruptions with Runaway Current Plateau Formation in JET and Implications for ITER

A. Loarte[1], V. Riccardo[2], J.R. Martin-Solís[3], J. Paley[4], A. Huber[5], M. Lehnen[5]
and JET EFDA contributors*

JET-EFDA, Culham Science Centre, OX14 3DB, Abingdon, UK

[1]ITER Organization, Route de Vinon, CS 90 046, 13067 Saint Paul Lez Durance, France
[2]Culham Centre for Fusion Energy, Euratom/UKAEA Fusion Association, Culham Science Centre, Abingdon, Oxon, OX14 3DB, UK
[3]Departamento de Física, Universidad Carlos III de Madrid, 28911 Leganés, Madrid, Spain
[4]Association EURATOM-Confédération Suisse, Ecole Polytechnique Fédérale de Lausanne (EPFL), CRPP, CH-1015 Lausanne, Switzerland
[5]Forschungszentrum Jülich GmbH, Institut für Plasmaphysik, EURATOM-Assoziation, Trilateral Euregio Cluster, D-52425 Jülich, Germany
** See annex of F. Romanelli et al, "Overview of JET Results", (Proc. 22 nd IAEA Fusion Energy Conference, Geneva, Switzerland (2008)).*

Preprint of Paper to be submitted for publication in
Nuclear Fusion

ABSTRACT.
The magnetic energy balance and magnetic energy flows for plasma disruptions in which runaway plateau plasmas are formed and terminated at JET has been analysed and compared to that of runaway-free disruptions. The analysis shows that the energy loss processes during runaway plateau plasma termination are qualitatively different from those of a runaway-free disruption because of the pre-existence of a runaway population in the first case. As a consequence, a significant fraction of the runaway plateau plasma magnetic energy is directly converted into runaway electron kinetic energy during the runaway plateau termination phase. This leads to the fluxes being deposited by runaway electrons onto in-vessel components during the termination of runaway plateaus to be significantly larger than those expected from the initial kinetic energy of the runaway electrons in the runaway plateau plasma.

1. INTRODUCTION.

In the next generation of burning plasma tokamaks, the plasma facing components will be subject to large energy fluxes during disruptions [24], which can reduce significantly their operational lifetime. The processes that dominate the flow of energy from the plasma to the in-vessel components for the two phases of the disruptions (thermal quench and current quench) have been studied and characterised in detail for JET [29, 1] and other tokamaks [3, 23] providing the physics basis for the evaluation of these fluxes for ITER [24, 16]. In present experiments, most of the disruptions occurring during normal plasma operation (i.e. excluding those intended to produce large runaway current plateaus) do not generate significant runaway tails during the current quench. On the contrary, due to the large plasma magnetic energy, large electric field during current quench and the longer duration of the current quench itself, significant runaway currents are expected to be routinely generated during disruptions in next step devices such as ITER [24]. Runaway electrons have been found to deposit their energy in very short pulses and in localised areas of the in-vessel components in present devices that can cause significant localised damage to these components (see for instance [20]).

Understanding the magnitude of the energy fluxes to in-vessel components in disruptions with runaway formation in present devices and their extrapolation to ITER has triggered a significant number of studies following the identification of the avalanche mechanism as dominant for the generation of runaways with increasing plasma current and tokamak size [31]. These experimental and modelling studies have concentrated mostly on the determination of the mechanisms that dominate runaway generation in present devices, their dependence on plasma conditions and their extrapolation to ITER with the goal of predicting the typical level of runaway current to be expected in ITER disruptions [35, 36, 5, 12, 28, 25, 17, 7, 32, 33]. On the contrary, detailed studies of the processes that dominate the energy balance and energy flows during runaway plateau plasma formation and, in particular, during their termination both from the experimental and theoretical points of view are scarce [26, 35, 36, 34, 2]. This is in contrast to the obvious importance of these

processes for the determination of the timescale and magnitude of the energy fluxes deposited by runaway electrons on in-vessel components when the runaway plateau plasmas are terminated.

This paper describes the analysis of the energy balance processes during the current quench of JET discharges with measurable runaway current plateaus. In this paper we concentrate on the analysis of the balance of magnetic energy because this is the dominant term in the total content of plasma energy both for the post-thermal quench plasma as well as for runaway plateau plasmas. It is important to note however, that the deposition of the kinetic energy of the runaway electrons and of the magnetic energy at the termination of the runaway plateau plasmas may take place over different timescales and with different spatial distributions leading thus to different power fluxes to in-vessel components. The discharges analysed in this paper comprise accidental disruptions in which runaway plateaus were generated as well as dedicated experiments in which runaway current plateaus were generated purposely (typically by the puffing of a large impurity influx) from JET operation between 1985 to 2009 [6, 30]. The range of pre-disruptive plasma currents in the discharges analysed is 1 - 6 MA and the corresponding runaway current plateaus are in the range of 0.3-3.0 MA. The discharges considered are all in limiter configuration; this is found to be favourable for the formation of runaway plateaus at JET because of the lower growth rate of the vertical instability that follows the disruption thermal quench [14].

The paper is organised as follows :

(a) Section 2 describes the typical experimental observations during the formation of runaway plateau plasmas and their termination at JET.

(b) Section 3 analyzes the energy balance during the formation of runaway discharges and their termination at JET including the flows of magnetic energy and the losses by plasma radiation.

(c) Section 4 analyzes the timescales of the processes involved in the termination of runaway plateaus at JET and their influence on the dominant mechanisms for the loss of magnetic energy of the runaway plateau plasma discharge.

(d) Section 5 describes modelling of runaway plateau formation and loss for JET discharges and discusses the experimental results described in sections 2-4 in the light of results of these simulations.

(e) Finally, section 6 extracts conclusions from the experimental and modelling findings from JET experiments and discusses their implications for ITER.

2. BASIC OBSERVATIONS OF DISRUPTIONS WITH FORMATION OF RUNAWAY PLATEAUS AND THEIR TERMINATION AT JET.

The experiments analysed in this paper correspond to discharges in limiter configuration which, following a disruption, generate runaway plateaus with typical durations of several 10's of ms. Both disruptions accidentally triggered and purposely triggered for disruption/runaway studies experiments are considered. Fig. 1 shows a JET experiment in which a Neon puff in the

main chamber is utilized to trigger the plasma disruption. Following the initial current quench in which the plasma current derivative is negative and very large (~100 MAs^{-1}) a runaway electron current plateau is formed. During the initial current quench and the runaway plateau formation phase the plasma experiences an inwards drift associated with the decrease of plasma pressure, which is then followed by a vertical drift as the runaway plasma becomes vertically unstable (upwards or downwards depending on the conditions; in the example of Fig. 1 the movement is downwards). During these phases the presence, position and extent of the runaway electron beam in the plasma can be identified by the soft X-ray emission produced by the interaction of the high energy electrons with impurity atoms in the thermal plasma that follows the initial current quench [5]. Finally, the runaway plasma becomes unstable and the runaway electrons are lost to the in-vessel components producing a peak in the measured electromagnetic radiated power from the plasma and the photoneutron emission as shown in Fig.1. After this, the remaining current in the post-runaway plasma decays in time scales of ~5ms. The peak in the plasma radiation at the runaway plateau termination is of much smaller magnitude than during the thermal quench and the initial current quench in the disruption and it is poloidally localized to the region where runaways are lost as shown in Fig. 2, in contrast to the radiation distribution in the current quench where it is distributed over a large volume of the plasma [10].

The formation of a runaway electron beam during the current quench has been postulated to lead to a peaking of the current profile from the soft-X ray observations described above [5], which is in good agreement with theoretical expectations [Smith 2006]. The magnitude of their current profile peaking, as characterised by the plasma internal inductance l_i (3) has been evaluated in JET by means of plasma equilibrium reconstruction with EFIT [13] through the current quench and the runaway plateau phases, with the assumption that the β_p (poloidal beta) of the plasma after the thermal quench is very small (~ 0). As shown in Fig. 3, at the start of the disruption the current profile experiences a strong flattening leading to the usual positive current spike by magnetic flux conservation [37]. Following this, the magnitude of the runaway current increases towards its plateau value and together with it the current profile itself peaks, as shown by the increase of the plasma internal inductance, reaching values which are typically in the range of 2 – 3 for JET and thus a factor of 2 – 3 times larger than those typical of pre-disruptive conditions.

Analysis of a wide database of JET discharges indicates that the change of the current density profile peaking, in relation to the pre-disruptive current density profile peaking, is correlated with the magnitude of the initial current derivative at the current quench, although the scatter in the database is large, as shown in Fig. 4. This indicates that the larger electric fields at the current quench, associated with the larger current derivatives, increase the peaking of the current profile, which is consistent with theoretical expectations [33]. Equilibrium reconstruction codes are not usually employed to perform reconstructions of runaway plasmas, for which measurements are intrinsically complex, and thus the results obtained can be subject to large uncertainties. Therefore, an independent estimate of the current profile peaking has been carried out by utilizing the

measurements of the soft X-ray emission during runaway plateaus at JET, as shown in Fig. 5, and by assuming that the soft X-ray emission is proportional to the runaway current. The width of the runaway current profile ΔZ_{curr} has been characterised by the full width of the soft X- ray emission profile peak at e^{-1} of its maximum. Utilizing ΔZ_{curr} and the plasma radius a, from the equilibrium reconstructions, the magnitude of the runaway current profile peaking has been calculated under the assumption that all the measured plasma current in the plateau phase is carried by the runaway electrons (i.e. $I_p = I_p^r$, where I_p is the plasma current and I_p^r is the runaway electron current) within a radius of $\Delta Z_{curr}/2$, within which an average current density of $j_{curr} = I_p^r/((\pi(\Delta Z_{curr}/2)^2)$ is assumed. For these simplifying assumptions, the internal inductance of the runaway plateau discharge can be quantified from the soft X-ray emission measurements by:

$$l_{i,X\text{-}rays} = 1/2 + 2\ \ln[a/(\Delta Z_{curr}/2)] \quad (1)$$

The runaway plasma internal inductance estimated in this way has been compared with that derived from equilibrium reconstructions for a set of JET discharges and it has been found to be in reasonable quantitative agreement; although large differences (factors of ~ 1.5-2) between the two estimates occur for some discharges. Fig. 6 shows a histogram of the results of such comparison illustrating that for about ~ 70% of the discharges analysed the estimates of l_i with both methods agree within ± 30%.

The increase of the plasma internal inductance during the formation of runaway plateau plasmas plays a role in the balance of magnetic energy following the thermal quench. Due to the increased current profile peaking, the magnetic energy of the runaway plasma can be substantially larger than what would be estimated in its absence and it can ultimately limit the maximum level of runaway current that can be generated in a disruption. The total plasma magnetic energy is given by

$$E_{mag} = ½\ L_p\ I_p^2 \quad (2)$$

where the total plasma inductance can be approximated by

$$L_p = \mu_0\ R_0\ (\ln(8R_0/a) - 2 + l_i/2) \quad (3)$$

For the typical values of the runaway plasmas analysed at JET and the range of the internal inductance in these runaway plasmas (l_i = 2-3), the runaway plasma magnetic energy is found to be ~ 25-50% larger than that estimated by assuming that the plasma current peaking of the runaway plasma is similar to that before the current quench (typically l_i ~ 1.0 - 1.2). In fact, the magnetic energy in runaway plateau plasmas at JET is found to be in the range of 15-50% of the pre-disruptive magnetic energy as shown in Fig. 7, demonstrating that for some cases a substantial amount of the pre-disruptive magnetic plasma energy is kept in the runaway plateau plasmas

which are formed after the initial phase of the current quench. The implications of this finding will be discussed in more detail in sections 3 and 4.

Runaway plateau plasma discharges become finally unstable and runaway electrons are lost in a series of bursts that can be identified by the emission of hard X-rays and photoneutrons caused by the interaction of the high energy electrons with the in-vessel components [36, 5]. The processes and instabilities that lead to the final loss of the runaway plateau plasma are not well understood : in some cases they can be connected to the movement of the runaway plasma (an example is described in Fig. 1) which terminates the discharge as the runaway plasma is compressed against the in-vessel components reducing its cross-section and triggering MHD instabilities [36]; in other cases, in which position control of the runaway plasma is maintained, it has been proposed that other MHD instabilities of the runaway beam itself (i.e. not dependent on their movement) are responsible for their termination [8]. Independent of the nature of the instability that terminates the runaway plateau plasma, it is experimentally found at JET that there is a large variability regarding the events that terminate them and in their timescales, as well as in the characteristics of the low temperature thermal plasma which is left after the runaway electrons are lost. Two typical examples of this variability are shown in Figs. 8 & 9. Fig. 8.a shows a discharge in which the final phase of runaway electrons loss takes place over an extended period (~ 10 ms) in a series of discrete events leading to large spikes in the hard X-ray and photoneutron measurements. Despite the significant runaway losses in every of these spikes, a measurable runaway electron population is found to exist in the plasma (from soft X-ray emission shown in Fig. 8.b) until the last spike in the hard X-ray and photoneutrons, in which the runaway population and the associated soft X-ray signal is found to vanish. At this time, the post-runaway thermal plasma carries a current which is only a small fraction of the initial runaway plateau plasma current (~30%). In other experiments, such as shown in Fig. 9.a, virtually all the runaway electrons are lost in one or few large events following which the associated soft X-ray signal is found to vanish, as shown in Fig. 9.b. In this case, the plasma current which circulates in the thermal plasma following the complete loss of runaway electrons is a large fraction of the initial runaway plateau current (~80%). For these conditions, the post-runaway thermal plasma can thus maintain a significant proportion of the magnetic plasma energy from that of the runaway plateau plasma. The connection between runaway loss timescales, the thermal level of plasma current after runaway loss and the implications for energy balance during runaway plasma termination are discussed in the following two sections.

3. ENERGY BALANCE FOR DISRUPTIONS WITH FORMATION OF RUNAWAY PLATEAU PLASMAS AND THEIR TERMINATION AT JET.

Studies of the energy balance and of the associated power fluxes during disruptions at JET and other devices have concentrated so far in runaway free disruptions and VDEs [27, 28, 1, 10, 3, 23, 21, 22]. For these cases, it has been found that the dominant mechanism for the loss of magnetic energy from the plasma during the current quench at JET is the emission of electromagnetic

radiation by partially ionised impurities in the thermal low temperature/high density plasma that follows the thermal quench [27, 21, 22]. In this section, we present the first analysis of energy balance and energy flows for disruptions at JET in which runaway plateau plasmas are formed following the initial current quench. For this analysis, we follow the methodology originally developed for DIII-D [9], which has been extensively applied to the analysis of the energy balance in runaway-free disruptions at JET [21, 22]. We describe briefly the approach below; more details can be found in the references [9, 21, 22].

The method for determining the magnetic energy flow and balance during disruptions at JET is based on the evaluation of the electromagnetic flow of plasma energy into the vacuum vessel during a disruption by the application of Poynting's theorem. The magnetic energy which is dissipated inside the vacuum vessel either by induction of currents on the vessel/in-vessel conductors or by the plasma (which loses the energy by radiation, conduction/convection or by direct deposition of runaway electrons onto in-vessel components), at a given time t in the disruption is given by:

$$E_{loss}^{total}(t) = E_{loss}^{plasma}(t) = E_{loss}^{conductors}(t) = W_{pol}(t_{ref}) + \frac{1}{\mu_0}\int_{t_{ref}}^{t}\int_{S} E_\phi B_\theta \, ds \qquad (4)$$

where E_{loss}^{total} is the total magnetic energy dissipated into the vacuum vessel in the temporal development of the disruption up to time t, E_{loss}^{plasma} is the magnetic energy dissipated by the plasma, $E_{loss}^{conductors}$ is the magnetic energy dissipated by the by induced currents in the vessel and in-vessel structures, W_{pol} (t_{ref}) is the poloidal magnetic energy inside the vessel (both in the plasma and between the plasma and the vacuum vessel) before the disruption at the reference time t_{ref} (which is chosen to be close to the disruption time but so that accurate magnetic equilibrium reconstruction can be performed) and the integral term is the influx or outflux of magnetic energy into the vacuum vessel during the temporal evolution of the disruption from t_{ref} up to time t.

For JET, there is usually an influx of magnetic energy into the vacuum vessel during a disruption; this is possible because the penetration time of the magnetic flux across the vacuum vessel at JET is ~ 4 ms and thus shorter than the typical current quench timescale [37]. The major contributor to the dissipation of magnetic energy in conducting structures during disruptions at JET has been found to be the vacuum vessel itself [29, 22] given its relatively high resistance (340 μΩ) [37]. The dissipation of magnetic energy into ohmic heating of the vacuum vessel itself can be determined from the measured loop voltage during the disruption and the vacuum vessel resistance. For the runaway plateau plasmas analysed, the dissipation of energy into ohmic heating of the vacuum vessel is of similar magnitude of the magnetic energy influx during the plasma current transients so that, typically, the magnetic energy available for dissipation into the plasma is similar to the initial poloidal magnetic energy inside the vessel at time t_{ref}. Fig. 10 shows a typical example of the magnitude and time evolution of the various terms in Eq. 4 terms, as well as of the instantaneous power fluxes during a discharge with runaway plateau formation and termination at JET. As explained above, both when the current quench is initiated and also when the runaway plateau

is terminated there is an influx of magnetic energy across the vessel most of which is dissipated by resistive heating of the vacuum vessel by induced currents in these phases. As a result, the magnetic energy that can be dissipated by the plasma is only somewhat higher than its initial value ($W_{pol}(t_{pre})$), typically by 10-20%. As shown in Fig. 10, most of the magnetic energy dissipated by the plasma in the initial current quench is in the form of plasma radiation, which is typical of JET disruptions without runaway plateaus. On the contrary, during the termination of the runaway plateau plasma the level of plasma radiation is very small, as well as the induced vessel currents in this phase. This demonstrates that the magnetic energy of the runaway plasma is deposited directly onto the in-vessel components (by runaway kinetic energy deposition or conduction/convection by the thermal plasma) and not by plasma radiation or by inductive current dissipation in the vessel.

The detailed energy balance analysis described above has been carried out for a series of discharges with runaway plateaus (and for runaway-free disruptions for comparison) separating the magnetic energy balance in Eq. 4 into two steps for the discharges with runaway plateaus : the initial current quench (step 1) and the runaway plateau termination (step 2), and evaluating the dissipation of plasma energy for these two steps separately. For the evaluation of the runaway plateau plasma magnetic energy contained inside the vacuum vessel ($W_{pol}(t_{ref\text{-}step\text{-}2})$), it is assumed that radiative losses are the dominant mechanism for magnetic energy loss during the initial current quench, as shown in Fig. 10 in agreement with previous JET experience [27, 21, 22], so that for the runaway plateau plasma:

$$W_{pol}(t_{ref-step-2}) = W_{pol}(t_{ref-step-1}) + \frac{1}{\mu_0} \int_{t_{ref-step-1}}^{t_{ref-step-2}} \int_s E_\phi B_\theta \, dS - E_{loss}^{conductors}(t_{ref-step-1}, t_{ref-step-2}) - E_{rad}(t_{ref-step-1}, t_{ref-step-2}) \quad (5)$$

where $E^{conductor}_{loss}$ and E_{rad} are the energy lost by dissipation in the conductors and radiated by the plasma in the initial current quench (i.e. for step 1 from $t_{ref\text{-}step\text{-}1}$ to $t_{ref\text{-}step\text{-}2}$), respectively. For the discharges considered in this detailed analysis, the runaway plateau magnetic energy contained inside the vacuum vessel is typically in the range ~ 30-75% of the initial in-vessel pre-disruptive magnetic energy. This is somewhat higher than the ratio estimated for the total magnetic energy of the runaway plasma with respect to pre-disruptive plasmas of ~ 15-50% (see Fig. 7). The reasons behind the difference of these two ratios are twofold : a) for conditions with high current profile peaking, such as those found for runaway plateau plasmas at JET, a larger proportion of the total plasma energy is contained inside the vessel than for broader current profiles, thus leading to a larger proportion of the total magnetic to be contained inside the vessel for runaway plateau plasmas than for normal pre-disruptive plasmas; this is not taken into account in the total magnetic energy analysis in Fig. 7 and b) there can be additional plasma conductive/convective losses during the initial current quench of discharges with runaway plateaus that could decrease the estimated in-vessel magnetic energy of the runaway plateau plasma from Eq. 5. On the basis of the comparison of these two different methods, we conclude that the in-vessel magnetic energy of the runaway plateau plasma estimated by our energy balance analysis above may be overestimated by at most a factor of 1.5-2.

Comparison of the radiative losses both during the initial current quench and the termination of runaway plateau discharges at JET with the in-vessel magnetic energy analysis of Eq.4 shows that the role of radiative losses in these discharges is quantitatively different from normal disruptions without runaway generation, as shown in Fig. 11. While losses by radiation in the current quench of disruptions without runaways can account for 50 - 100% of the in-vessel magnetic energy, they can only account for typically less than 50% of the losses for the initial current quench in discharges in which runaways are formed. This is consistent with a significant fraction of the initial pre-disruption magnetic energy remaining in the runaway plateau plasma after the initial current quench. More surprising is the fact that radiative losses are negligible (< 10% of the in-vessel magnetic energy) at the termination of the runaway plateau plasmas. Given the major importance of this finding, the small the role of radiative losses in the termination of runaway plateau plasmas at JET has been confirmed by the analysis of the total magnetic energy balance of a wider database of runaway-free disruptions and of runaway plateau terminations by the application of some simplifying assumptions based on the results of section 2. For this wider database, the total magnetic energy of the plasma has been evaluated in an approximate way : l_i =1.2 is assumed for pre-disruptive plasmas in runaway-free disruptions and l_i =2.5 is assumed for runaway plateau plasmas. The total magnetic energy thus estimated is compared with the integrated energy lost by radiation in the whole current quench phase of the runaway-free disruptions and in the runaway plateau termination phases. Fig. 12 shows the results of the analysis of the total magnetic energy of runaway plateau plasmas and the radiative losses at their termination confirming the findings from the in-vessel magnetic energy analysis for a smaller set of discharges; radiative losses during runaway plateau terminations are markedly lower than those found during the current quench of runaway-free disruptions also when the total plasma magnetic energy is considered.

These results show that the processes involved in the loss of magnetic energy from a runaway plasma are qualitatively different from those in the current quench that follows the thermal quench of plasma disruptions. These processes will be described in more detail in sections 4 and 5.

4. TERMINATION CHARACTERISTICS AND MAGNETIC ENERGY LOSS OF RUNAWAY PLATEAU PLASMAS AT JET.

As discussed above and shown in Figs. 8 and 9, the termination of runaway plateau plasmas is associated with the sudden loss of runaway electrons caused by the instability of the runaway plasma discharge. This instability leads not only to a deposition of the runaway electrons kinetic energy by their impact onto the in-vessel components but also to a decrease of the plasma current (mostly carried by runaway electrons), as runaway electrons are lost. This plasma current decreases leads, in turn, to an increase of the electric field on the plasma discharge which can eventually lead to a further generation of runaway electrons and the direct conversion of the magnetic energy of the runaway plateau plasma into runaway electron kinetic energy as originally identified in [26]. The electric field created by the initial loss of runaways acts both on the remaining runaway

electron population and on the thermal plasma formed after the disruption thermal quench that surrounds the runaway electrons plasma. The electric field thus generated can have two effects on the plasma discharge : a) it can lead to the further generation of additional runaway electrons and/ or b) can induce an ohmic current in the thermal plasma, as shown schematically in Fig. 13.

From this basic physics picture, the balance of the processes involved in the final loss of the runaway plateau plasma magnetic energy should be dependent on the timescales of the runaway loss process, as this drives the appearance of the electric field in first place, and on the thermal plasma characteristics (i.e. its resistivity), as these determine the magnitude of the plasma current that can be induced in the thermal plasma by the electric caused by the runaway electron loss. It is thus important to experimentally characterise the timescales of these processes and the characteristics of the thermal plasma in order to determine whether the above physics picture is valid and if it can explain the large variations measured in the magnetic energy left in the plasma after runaway electrons are lost (as shown by the plasma current in Figs. 8 and 9). For this purpose a set of discharges JET has been analysed with formation of runaway plateaus with pre-disruptive plasma currents in the range of 1-6 MA and runaway plateau currents in the range of 0.5-3 MA, as shown in Fig. 14.

For the systematic characterisation of changes in the plasma current and of the loss of runaway electrons in runaway plateau terminations, the following parameters have been defined (see Fig. 15):

a) The timescale for plasma current decay (Δt_{Ipr}) has been defined, following a similar approach to that applied to disruptions without runaway formation, as the time that it takes the plasma current to decay from 0.9 I_p^r to 0.2 I_p^r, where I_p^r is the runaway plateau plasma current value.

b) The duration of the period over which the losses of runaways take place ($\Delta t_{neut\text{-}X\text{-}rays}$) is determined by the time interval between the first and the last peak in the photo-neutron and hard x-ray emission during the runaway plateau termination phase.

c) Because runaway electrons are lost in several short events, the characteristic timescale for the loss of runaway electrons can be much shorter that the period over which they are lost ($\Delta t_{neut\text{-}X\text{-}rays}$). In order to account for this fact, the following definition for the typical timescale for runaway electron loss from the photoneutron emission measurements (τ_{neut}) has been adopted, $t_{neut} = \frac{\int I_{neutrons}}{I_{neutrons}^{\max}}$. For experiments in which runaway electrons are lost predominantly in one event τ_{neut} corresponds to the duration of the dominant runaway loss event, i.e. $\tau_{neut} \sim \Delta t_{neut\text{-}X\text{-}rays}$.

d) The level of the measured plasma current after the majority of the runaway electrons are lost (I_p^{aft}) is defined as $I_p^{aft} = I_p(t = \Delta t_{neut\text{-}rays})$. I_p^{aft} is directly correlated with the magnetic energy which is left in the plasma after the runaway electrons are lost onto in-vessel components. The characteristic timescale for the decrease of the plasma current in

the post-runaway plasma ($t_{c.q.}^{aft}$) is defined by utilizing the time derivative of the post-runaway plasma current as $t_{c.q.}^{aft} = |I_p^{aft}/(dI_p/dt)|_{aft}|$, where $(dI_p/dt)|_{aft}$ is the maximum plasma current time derivative of the post-runaway plasma

The timescales obtained with this methodology are shown in Fig. 16.a, in which τ_{neut} and $\Delta t_{neut-xrays}$ are plotted versus Δt_{Ipr}. The results in Fig. 16.a reveal that for most cases at JET, the timescale of runaway loss (τ_{neut}) is much shorter than the period over which the runaway loss takes places ($\Delta t_{neut-xrays}$). This has significant implications for the energy balance of runaway plateau plasma terminations, as will be discussed below. Fig. 16.a also shows that the timescale for runaway plateau plasma current termination (Δt_{Ipr}) is not an appropriate parameter for the characterisation of the timescale of runaway electron loss, as it is determined by both the duration of the period over which runaways are lost ($\Delta t_{neut-xrays}$) and also the behaviour of the post-runaway plasma current (i.e. the timescale for the decay of I_p^{aft}, $t_{c.q.}^{aft}$). No correlations with measurable parameters of the runaway plateau plasmas nor of the pre-disruptive plasmas have been found for either τ_{neut} or $\Delta t_{neut-Xrays}$; as an example both parameters are plotted versus the runaway plateau plasma current in Fig. 16.b.

The magnitude of the plasma current which is carried by the thermal plasma after the runaway electrons are lost, I_p^{aft}, is found to be in the range of 20 - 100 % of the runaway plateau plasma current I_p^r, as shown in Fig. 17, illustrating the large variability in the conversion of magnetic plasma energy from the runaway plateau plasma ($\sim (I_p^r)^2$) into magnetic energy of the post-runaway plasma ($\sim (I_p^{aft})^2$). From the physics picture described above, it is expected that the efficiency of transformation of runaway electron current into ohmic plasma current in the thermal plasma should increase with the electric field created by the loss of runaway electrons and with decreasing plasma resistance of the thermal plasma as $I_p^{aft} \sim E_\phi/R_{aft}$.

The effective plasma resistance of the thermal plasma can be evaluated in an approximated way from the timescale of current decay in the post-runaway thermal plasma, in a similar way to that during the current quench of runaway-free disruptions, as:

$$t_{c.q.}^{aft} = |I_p^{aft}/(dI_p/dt)|_{aft}| = L_{aft}/R_{aft} \quad (6)$$

where L_{aft} is the plasma inductance of the post-runaway thermal plasma and R_{aft} its resistance. Comparison of the $t_{c.q.}^{aft}$ timescale with that of the initial current quench in JET disruptions with a runaway plateau (calculated in an analogous way to that in Eq. 6) shows that, in most cases, the timescale of the initial current quench is longer than $t_{c.q.}^{aft}$ (see Fig. 18). This lower timescale for the current decay in the post-runaway plasma is unlikely to be due to a lower plasma inductance for the post-runaway plasma than that for the initial phase of the current quench because during the initial phase of the current quench the current profiles are already very broad ($l_i \sim 0.7$ as shown in Fig. 3) and it is thus unlikely that the post-runaway profiles will be much broader. It is

therefore concluded that the effective plasma resistance of the post-runaway thermal plasma must be higher than that of the plasma during the initial current quench. It is important to note that the plasma resistance of the thermal plasma during the runaway loss phase itself is likely to be higher than that during the post-runaway phase because of the lower of ohmic plasma current and ohmic heating of the thermal plasma during the runaway loss phase. The estimates performed here on the basis of the experimental measurements available intend to provide a guideline to interpret the experimental results but detailed modelling is required to extract quantitative conclusions from these measurements, as described in section 5 and in future publications [14, 19].

The average electric field generated by the loss of runaway electrons is proportional to the derivative of the runaway current during the runaway loss phase. This derivative can be approximated from the initial runaway plasma current (I_p^r) and the timescale for runaway loss (τ_{neut}) as $|dI_p^r/dt| \sim I_p^r/\tau_{neut}$, under the assumption that the majority of the plasma current during the runaway plateau phase is carried by runaway electrons. Thus the electric field induced by the loss of runaway electrons can be approximated by

$$E_\phi = - 1/(2\pi R_0) L dI_p^r/dt \sim I_p^r/\tau_{neut} \quad (7)$$

With these approximations and the physics picture described above, the proportion of runaway current which is transformed into ohmic plasma current in the post-runaway plasma is given by

$$I_p^{aft}/I_p^r \sim E_\phi/(R_{aft} I_p^r) \sim t_{c.q.}^{aft}/\tau_{neut} \quad (8)$$

The experimental database analysed (see Fig. 19) supports the trend of increasing I_p^{aft}/I_p^r with $t_{c.q.}^{aft}/\tau_{neut}$, although there remains a significant scatter. For low values of $t_{c.q.}^{aft}$ the ratio I_p^{aft}/I_p^r can be as low as ~ 0.2, while for high values of $\sim t_{c.q.}^{aft}/\tau_{neut}$ the ratio I_p^{aft}/I_{pr} is in the range ~ 0.4-0.75, with few discharges reaching ~ 0.95.

Although it has not been possible to determine the current profile peaking of the post-runaway plasma by equilibrium reconstruction, it is not likely that the current profile in the initial phase of the post-runaway plasma (i.e., when the plasma current is close to I_p^{aft}) is more peaked than during the runaway plateau itself, i.e., $L_{runaway} \geq L_{aft}$, where $L_{runaway}$ and L_{aft} are the plasma inductances for the runaway plateau plasma and the post-runaway plasma respectively. As we have shown in section 2, runaway plasmas have very peaked current profiles; the ohmic current induced in the post-runaway plasma by the electric field originated from the runaway loss diffuses inwards from the plasma edge thus leading to flat ohmic current profiles, at least in the initial phases of this diffusion, as shown by modelling in section 5. Taking into account the expected behaviour of the plasma inductance and the measured plasma currents in the runaway plateau plasma (I_p^r) and in the post-runaway plasma (I_p^{aft}), it is possible to provide a lower estimate for the total runaway plateau plasma magnetic energy which is dissipated by the plasma during the runaway loss phase,

$\Delta t_{neut\text{-}xrays}$, as

$$\Delta E_{mag} = E_{mag}^{r} - E_{mag}^{aft} = \tfrac{1}{2} L_{runaway} (I_p^{r})^2 - \tfrac{1}{2} L_{aft} (I_p^{aft})^2 \geq \tfrac{1}{2} L_{runaway} [(I_p^{r})^2 - (I_p^{aft})^2] \quad (9)$$

where E_{mag}^{r} and E_{mag}^{aft} are the total magnetic energies of the runaway plateau plasma and the post-runaway plasma respectively. Fig. 20 shows the normalised (to the total runaway plateau magnetic energy) magnetic energy loss during $\Delta t_{neut\text{-}xrays}$ for the JET discharges analysed. In most cases, a large fraction of the runaway plateau magnetic plasma energy (> 50%) is also lost in the period in which runaway electrons themselves are lost. As we have shown in sections 2 and 3, the radiation losses during this phase are small as well as the losses associated with the induction of currents in the vacuum vessel. Therefore, we can conclude that for most of the runaway plateau plasma terminations at JET a substantial fraction (> 50%) of the initial runaway plateau plasma magnetic energy is directly deposited onto the in-vessel during the period in which runaway electrons are lost. This magnetic energy deposition is in addition to the initial kinetic energy of the runaway electrons in the runaway plateau plasma which is also deposited onto the in-vessel components during this phase. After the runaway electron loss phase is over, the remaining magnetic energy in the post-runaway plasma will also deposited by conduction/convection onto the in-vessel components from the thermal plasma, given the low radiation losses during the termination phase of runaway plasmas in JET, with typical timescales characterised by $t_{c.q.}^{aft}$.

Direct experimental evidence for the conversion of runaway plasma magnetic energy into runaway electron kinetic energy has been obtained from the analysis of the integrated neutron count for discharges with runaway plateaus and its correlation with the duration of the runaway plateau phase ($t_{plateau}$) and the characterise current decay time in the initial phase of the disruption $t_{c.q.} = |I_p/(dI_p/dt)|_{c.q.} = L_{c.q.}/R_{c.q}$, during which a large electric field is produced in the disruption leading to the formation of the initial runaway population. For typical conditions at JET, the integrated neutron emission associated with the deposition of runaways is proportional to the total energy of deposited by runaways on in-vessel components [Jarvis 1988]. In the absence of an additional conversion of magnetic energy of the runaway plateau plasma into kinetic energy during the termination phase the following behaviour would be expected; for discharges with runaway plateau phases which are shorter than $t_{c.q.}$ an increase of the total runaway kinetic energy (and integrated neutron emission) is expected with increasing duration of the plateau phase as a larger proportion of the pre-disruptive magnetic energy can be converted into runaway kinetic energy within $t_{c.q.}$, during which the electric field on the plasma is significant. Once the duration of the runaway plateau exceeds $t_{c.q.}$, the magnitude of the electric field on the plasma is negligible and thus no further increase of the runaway kinetic energy and of the corresponding integrated neutron emission is expected for $t_{plateau}/t_{c.q.} > 1$. On the contrary, the experimental measurements show a continuous increase of the integrated neutron yield (and total runaway kinetic energy deposited onto in-vessel components) up to very large values of $t_{plateau}/t_{c.q.}$, as shown in Fig. 21. This indicates that there

is another mechanism leading to the increase of the kinetic energy which is deposited by runaway electrons onto the in-vessel components beyond the initial conversion of plasma magnetic energy into kinetic runaway energy at the disruption initial current quench. Fig. 21 also shows that the energy deposited by runaways onto in-vessel components can be significantly larger (by up to a factor of 10 in some cases) than the maximum that they can acquire during the initial current quench (i.e. for discharges in which $t_{plateau} \sim t_{c.q.}$).

For most runaway plateau plasmas, the initial kinetic energy of the runaway electrons is small compared to the magnetic energy of the runaway plateau plasma itself (typically ~ 10 - 30%). Therefore, understanding in detail the physics mechanisms that govern the conversion of the magnetic energy of the runaway plateau plasma into energy deposited onto the in-vessel components is required in order to perform a correct evaluation of the magnitude of the energy fluxes to in-vessel components during runaway plateau terminations and of their timescales in present devices and to provide a physics-basis for their evaluation in ITER. It is thus necessary to identify and quantify : a) the processes that determine the conversion of magnetic energy of the runaway plateau plasma into magnetic energy of the thermal plasma, b) the processes that cause the loss of a significant fraction of the initial magnetic energy of the runaway plateau plasma onto the in-vessel components during the duration of the electron runaway loss phase ($\Delta t_{neut\text{-}Xrays}$) and c) in which form is the magnetic energy deposited onto the in-vessel components during the runaway electron loss phase. This will be studied by the application of a simple model for runaway formation and loss to typical JET conditions and by detailed simulations of few typical JET runaway plateau plasma terminations in section 5.

5. MODELLING AND IDENTIFICATION OF THE MAGNETIC ENERGY LOSS PROCESSES FOR RUNAWAY PLATEAU PLASMAS TERMINATION AT JET.

Modelling of the termination of JET runaway plateau plasmas has been carried out with a model previously used to simulate the behaviour of runaway discharges in various tokamaks by solving the plasma current profile evolution with the contribution of the various runaway production mechanisms in a self consistent way [17, 18]. The details of the model can be found in [17, 18, and references therein] and it will only be briefly described here.

The evolution of the plasma current density (j_p) is evaluated by the solving the current diffusion equation in a plasma with a runaway component which can be written as

$$\mu_0 \frac{\partial j_p}{\partial t} = \frac{1}{r}\frac{\partial}{\partial r}\left[r \frac{\partial E_{\|}}{\partial r} \right] = \frac{1}{r}\frac{\partial}{\partial r}\left[r \frac{\partial \eta (j_p - j_r)}{\partial r} \right] \qquad (10)$$

where η is the plasma resistivity and j_r is the runaway electron current density. The runaway electron current density is given by the sum of the primary (Dreicer) electrons and the secondary avalanche electrons (which has a characteristic avalanche timescale of τ_s [31]) and the loss of runaway electrons with characteristic timescale τ_{diff} :

$$\frac{\partial j_r}{\partial t} = ecn_e \nu_{coll} \lambda + \frac{j_r}{\tau_s} - \frac{j_r}{\tau_{diff}} \quad (11)$$

This model has been applied to representative discharges for generation and loss of runaway plateau plasmas at JET (starting from plasma conditions after the thermal quench) by adjusting the level of plasma density and temperature of the thermal plasma after the thermal quench to match the measured plasma current evolution. For simplicity, the simulations assume that the plasma is surrounded by a perfectly conducting vessel so that only the in-vessel magnetic energy plays a role in runaway plateau plasma formation and loss. Although this assumption is not a realistic assumption for JET, which has a highly resistive vacuum vessel [37], it turns out that the magnetic energy influx into the vacuum vessel during these phases is approximately compensated by resistive losses in the vacuum vessel in these experiments, as shown in Fig 10, so that, in effect, the magnetic energy balance situation during runaway plateau plasma discharges and their termination at JET is not very different from that expected for a perfectly conducting vacuum vessel.

An example of a simulation for a 6 MA plasma disruption at JET leading to the formation of a runaway plateau plasma with 2 MA of runaway current (conditions similar to those in Fig. 14) are shown in Fig. 22.a-d. The first current quench leads to the appearance of a large electric field which in turn leads to the formation of large runaway current in a timescale of ~ 10 ms as shown in Fig. 22.a. During this phase no losses of runaway electrons are assumed to take place. Simultaneous with the runaway electron current formation, the current profile becomes much more peaked than at the beginning of the current quench reaching values of internal inductance of $l_i \sim 2.3$ during the plateau phase (see Fig. 22.b) , which is typical in JET discharges, as shown in Fig. 3. The evolution of the internal magnetic energy during this runaway formation phase is shown in Fig. 22.c. For this simulation, the runaway plateau plasma maintains about 8.5 MJ of internal magnetic energy from the initial 27.5 MJ at the beginning of the current quench, i.e. about 30% of the initial internal magnetic energy, which is well within the range observed at JET (see Fig. 7). As shown below (in Fig. 22.d), of the 19 MJ of magnetic energy lost in the initial current decay 3 MJ are converted into kinetic energy of the runaway electrons and the remaining 16 MJ are dissipated ohmically in the thermal low temperature plasma formed after the thermal quench, which is assumed to have a temperature of 10 eV in this example. If all the magnetic energy dissipated into ohmic heating during the initial current quench would be radiated, it would correspond to a level of radiated energy loss of ~ 60%, which is in the upper range of the observations for this phase of runaway discharges at JET, as shown in Fig. 11. The final phase of the runaway plateau discharge corresponds to its termination, which is modelled by the inclusion of a loss term for runaway electrons with a characteristic time of $\tau_{diff} \sim 1$ ms. As seen in Fig. 22.a, this leads to the complete loss of the runaway electrons in a time interval of ~ 7 ms during which a significant plasma current (~ 1.5 MA) is induced in the thermal ~ 10 eV plasma which surrounds the runaway plasma. In fact, the timescale for the decrease of the current carried by runaway electrons in this simulation

is significantly longer than τ_{diff}. This is due to the fact that the electric field created by the initial loss of the runaway electrons does not only lead to the induction of an ohmic current in the thermal plasma but also to the further generation of additional runaway electrons thus slowing down the runaway electron current decay itself, as proposed in the physics picture introduced in section 4. A major consequence of the generation of additional runaway electrons during the termination of the runaway plateau is that part of the initial magnetic energy of the runaway plateau plasma is converted into runaway electron kinetic energy, as shown in Fig. 22 d. For this simulation, about ~ 2.2 MJ from the initial plasma runaway plateau magnetic energy of ~ 8.5 MJ are converted into runaway electron kinetic energy at the termination of the runaway plateau. The remaining ~ 6.3 MJ are converted into ohmic heating of the thermal plasma during the runaway loss phase and into magnetic energy of the post-runaway plasma, which is finally dissipated ohmically as well. When both the initial runaway electron generation and loss phases are taken into account, the total conversion of pre-disruptive magnetic energy into runaway electron kinetic energy which will be deposited onto in-vessel components amounts to ~ 5.2 MJ. This is a factor of ~ 1.7 larger than that estimated by the usual analysis based on runaway electron formation which only considers the evolution of the plasma up to the runaway plateau but does not consider the runaway loss phase [17, 33].

The proportion of the runaway plateau plasma magnetic energy that is converted into runaway kinetic energy is strongly dependent on the timescale of the runaway loss process and on the resistivity (or plasma temperature) of the thermal plasma, as expected from the physics picture introduced in section 4. The resistivity of the thermal plasma influences the evolution of the electric field created by the runaway loss process, which in turn determines the generation further runaways. The timescale of the runaway process itself influences whether the losses of runaways exceed their generation rate under the electric field acting on them and thus the conversion of magnetic energy of the runaway electron plasma into runaway electron kinetic energy. A parametric study of the sensitivity of the magnetic to kinetic energy conversion during the termination of runaway plateaus at JET has been carried out for various assumptions regarding the level of plasma current in the runaway plateau, the thermal plasma temperature and the characteristic timescale for runaway loss. The results of this study are shown in Fig. 23.a and b. For JET, for which the typical runaway loss time from the photo-neutron emission is in the range of 0.5-3 ms (including subsequent runaway electron generation, see Fig. 16), the conversion of runaway plateau magnetic energy into runaway kinetic energy is in the range of 20 to 60%. The conditions for more efficient conversion correspond to the longest timescales for runaway loss and the lowest thermal plasma temperatures, as expected. Because the magnetic energy of the runaway plateau plasma in JET is typically a factor of ~ 3-10 times larger than the runaway electron kinetic energy, a conversion rate from magnetic to kinetic energy of 60% during the runaway plateau termination implies that the total amount of energy deposited by runaway electrons onto the in-vessel components is at least a factor of ~ 3 times larger than that usually estimated from the evaluation of the kinetic

energy of the runaway electrons in the plateau phase alone. When the transformation of magnetic energy of the runaway plateau plasma into kinetic energy of the runaway electrons is effective, the energy deposited by runaway electrons onto in-vessel components is expected to scales as ~ $(I_p^r)^2$ (i.e. with the runaway plateau plasma magnetic energy) rather than with ~ (I_p^r) (i.e., the plateau runaway electrons kinetic energy).

Because the detailed characteristics of the runaway loss process and of the thermal plasma are so critical for the determination of the efficiency of runaway magnetic energy conversion into runaway electron kinetic energy, simulations have been performed to reproduce in detail the timescales of the various runaway loss events for some JET discharges. The systematic study of a large set of JET discharges will be reported in a future publication [Martin-Solis 2010]; here we only describe the results for two extreme cases studied. One case corresponds to a runaway plateau plasma discharge in which runaway electrons are mostly lost in a single dominant event and whose thermal plasma temperature is estimated to be ~ 9 eV (Fig. 24.a and b corresponding to the discharge in Fig. 14). The other case corresponds to a runaway plateau plasma discharge in which runaway electrons are lost over an extended period in a series of events (Fig. 25.a and b corresponding to the discharge in Fig. 8) with a lower thermal plasma temperature (~5 eV). For these simulations, the number of runaway electron loss events, their duration (τ_{spike}, characteristic timescale for the duration of each runaway electron loss event) and the interval between events (Δt_{spike}) is taken from experimental measurements of photoneutron emission. The timescale of the runaway loss process in each photoneutron spike and the thermal plasma temperature is adjusted in the model to reproduce the total plasma current evolution and its derivative during the termination of the runaway plateau and of the post-runaway plasma. As shown in Fig. 24.a and b, for conditions in which runaway electrons are lost in a single short event and the thermal plasma temperature is relatively high, most of the initial magnetic energy in the runaway plateau plasma is transformed into magnetic energy and ohmic heating of the thermal plasma and only 18% of the initial runaway plateau plasma magnetic energy is transformed into kinetic runaway electron energy. On the contrary, for the case in which runaway electrons are lost in many events over an extended period and in a thermal plasma with a lower plasma temperature (Fig. 25 a. and b.) it is found that the runaway electron population is partially recovered after every loss event by the generation of additional runaway electrons. This leads to most of the runaway plateau plasma magnetic energy to be transformed into kinetic runaway electron energy (81 %) by the end of the plateau termination phase.

6. DISCUSSIONS AND IMPLICATIONS FOR ITER.

The analysis of experimental measurements at JET and supporting modelling described in this paper demonstrates that the processes leading to the termination of runaway plateau plasmas are fundamentally different from those occurring during the current quench in runaway-free plasma disruptions because of the pre-existence of a runaway electron population. In JET runaway-free

disruptions, the plasma magnetic energy is ohmically dissipated into the low temperature plasma following the thermal quench and finally lost predominantly by plasma radiation from the impurities that enter the plasma following the thermal quench. For JET disruptions in which a significant population of runaway electrons is formed, the level of plasma radiative losses at the initial current quench is lower, as expected from magnetic energy conservation. In the termination of runaway plateau plasmas, the pre-existence of a runaway electron population in the background thermal low temperature plasma drastically changes the way in which the magnetic plasma energy is lost. Depending on the thermal plasma conditions and the timescales of the instabilities leading to the termination of the runaway plateau plasma, the magnetic energy in the runaway plateau plasma can be transformed into kinetic energy of runaway electrons by subsequent runaway electron generation or into magnetic energy and ohmic heating of the thermal plasma which surrounds the runaway electron plasma beam. In either case, the magnetic energy of the runaway plateau plasma is predominantly deposited onto the in-vessel components either by direct deposition of the runaway electron kinetic energy or by conduction/convection of the energy out of the thermal plasma, as radiative losses during these runaway termination phases are found to be very small.

From the point of view of the integrity of in-vessel components, the transformation of magnetic energy into runaway electron kinetic energy and their loss onto these components is the most unfavourable scenario :

a) in first place, because of their high energy, runaway electrons deposit the energy deeper into the component which poses a higher damage risk, particularly for components with thin plasma facing material cladding, such as water cooled components [20], and
b) the deposition of kinetic energy by runaway electrons is expected to be very localised onto the most protruding components. On the contrary, energy deposited by conduction/ conduction along the field lines from the thermal ohmic plasma that follows the runaway loss phase is expected to be deposited over much larger areas. These expectations are based on the edge transport properties of limiter discharges at JET and the inverse dependence with plasma current of the scrape-off layer width found in these experiments [4]. The plasma edge transport properties of these low temperature post-runaway thermal plasmas are unknown but they are expected to be very turbulent given the terminal stage of the plasma discharge. In this case, energy fluxes are likely to be spread over much larger areas than those deduced from conventional ohmic limiter discharges in JET [4].

Extrapolation of the results obtained at JET to ITER is subject to large uncertainties given our incomplete understanding and the incomplete measurements of runaway electron plasmas and thermal plasma characteristics. In general, modelling shows that for similar assumptions regarding the thermal plasma temperature and timescale for runaway loss, the conversion of magnetic energy of the runaway plateau plasma into runaway electron kinetic energy is less effective in ITER than in JET as shown in Fig. 26. This is due to the fact that, under these assumptions, the electric field generated by the initial decrease of the runaway current is proportional to the magnitude of

the runaway current itself (i.e., a factor of ~ 4-5 times larger in ITER compared to JET). Higher electric fields during the runaway loss phase favour the induction of ohmic currents in the thermal plasma and thus a less efficient conversion of magnetic energy into runaway electron kinetic energy for a given runaway loss timescale. From the detailed modelling of the JET discharges in Fig. 24 and 25, it is clear that simulations done with average runaway loss times to represent the whole runaway plateau termination, such as those done in Fig. 26, only provide guidance on the magnitude of this conversion. A precise evaluation of the magnetic to runaway electron kinetic energy conversion efficiency in ITER requires a detailed specification of the number, timescales and time intervals of the foreseen runaway loss events in the runaway plateau termination which are obviously difficult to predict at this stage. Despite these uncertainties, the analysis presented in this paper shows that for a large range of conditions in JET and also for ITER the conversion of few tenths of the runaway plateau magnetic energy into runaway electron kinetic energy is likely to take place and that this should be considered in the evaluation of the runaway electron loads onto in-vessel components. For discharges in which the runaway plateau current is a significant fraction of the pre-disruptive plasma current (i.e. low radiative losses in the first current quench) and thus with a high runaway plasma magnetic energy, as assumed for ITER 15 MA scenarios in Fig. 26, the total loss of runaway electron kinetic energy to in-vessel components during runaway plateau plasma termination can thus be significantly higher (by factors of 2 or more) than that estimated by accounting for the kinetic energy of the runaway electrons in the plateau phase alone.

Further progress in this area requires more detailed modelling studies of the runaway loss processes and their dependence on plasma characteristics but also improved measurements of the runaway electron plasmas as well as of the thermal plasmas for discharges with runaway plateaus at JET. For extrapolation of the JET results to ITER it is necessary to carry out similar analysis for other tokamaks. This is essentially required to determine the scaling with device size or with the runaway plateau plasma current of the thermal plasma properties (in particular its temperature) and of the timescales for the runaway loss events. Both characteristics have a crucial influence in the transformation of the runaway plasma magnetic energy into runaway electron kinetic and thus of major importance for the evaluation of energy fluxes to in-vessel components for disruption with runaway formation in ITER.

ACKNOWLEDGEMENTS

B. Esposito, L. Zabeo, G. Arnoux, D. Campbell, S. Putvinski and M. Sugihara are acknowledged for enlightening discussions on runaway electron physics and on the interpretation of the experimental measurements. This work was supported by EURATOM and carried out within the framework of the European Fusion Development Agreement. The views and opinions expressed herein do not necessarily reflect those of the European Commission.

REFERENCES.

[1]. Arnoux, G., et al., Nucl. Fusion **49** (2009) 085038.

[2]. Arnoux, G., et al., Proc 19th PSI Conference, San Diego, USA, 2010. To be published in J. Nuc. Mat.
[3]. Counsell G.F., et al., "Distribution of thermal energy during disruptions on MAST". Proc. 31th EPS Conf. on Controlled Fusion and Plasma Physics (London, UK, 2004) P-4.185.
[4]. Erents, S.K., et al., Nucl. Fusion **26** (1986) 1591.
[5]. Gill R.D., et al., Nucl. Fusion **42** (2002) 1039.
[6]. Harris G.R., "Comparison of the current decay during carbon-bounded and beryllium-bounded disruptions in JET". JET Joint Undertaking Report JET-R(90)07.
[7]. Helander, P., et al., Phys. Plasmas **11** (2004) 5704.
[8]. Helander, P., et al., Phys. Plasmas **14** (2007) 122102.
[9]. Hyatt, A.W., et al., "Magnetic and thermal energy flow during disruptions in DIII-D". Proc. 23rd EPS Conference on Plasma Physics and Controlled Fusion (Kiev, Ukraine, 1996). P.33.
[10]. Huber, A., et al., J. Nucl. Mat. **390-391** (2009) 830.
[11]. Jarvis, O.N., et al., Nucl. Fusion **28** (1988) 1981.
[12]. Kawano, Y., et al., Fusion Sci. Technol. **42** (2002) 298.
[13]. Lao, L., et al., Nuclear Fusion **25** (1985) 1421.
[14]. Lehnen, M., et al., J. Nucl. Mat. **390-391** (2009) 740.
[15]. Lehnen, M., et al., to be published.
[16]. Loarte, A. et al., "ELMs and disruptions in ITER : Expected Energy Fluxes on Plasma-Facing Components from Multi-machine Experimental Extrapolations and Consequences for ITER Operation". Proc. 21st Int. Conf. on Fusion Energy 2006 (Chengdu, China, 2006) (Vienna: IAEA) CD-ROM file IT/P1-14.
[17]. Martin-Solis, J.R., et al., Phys. Plasmas **7** (2000) 3369.
[18]. Martin-Solis, J.R., et al, Phys. Rev. Lett. **97** (2006) 165002.
[19]. Martin-Solis, J.R., to be published.
[20]. Nygren, R., et al., J. Nucl. Mat. **241-243** (1997) 522.
[21]. Paley, J.I., et al., J. Nucl. Mater. **337–339** (2005) 702.
[22]. Paley, J.I., "Energy flow during disruptions". Phd Thesis, Imperial College London, UK, 2006.
[23]. Pautasso G., et al., "Details of power deposition in the thermal quench of ASDEX Upgrade disruptions Proc. 31th EPS Conf. on Controlled Fusion and Plasma Physics (London, UK, 2004) P-4.132.
[24]. Progress on ITER Physics Basis, Nucl. Fusion **47** (2007) S203.
[25]. Plyusnin, V.V., et al., Nucl. Fusion **46** (2006) 277.
[26]. Putvinski, S., et al., Plasma Phys. Control. Fusion **39** (1997) B157.
[27]. Riccardo, V., et al., Plasma Phys. Control. Fusion **44** (2002) 905.
[28]. Riccardo V., Plasma Phys. Control. Fusion **45** (2003) A269.
[29]. Riccardo, V., et al., Nucl. Fusion **45** (2005) 1427.

[30]. Riccardo, V., et al., Proc. 37th EPS Conference on Plasma Physics, Dublin, Ireland, 2010. To be published in Plasma Phys. Control. Fusion.
[31]. Rosenbluth, M.N. and Putvinski, S.V., Nucl. Fusion **37** (1997) 1355.
[32]. Smith, H., et al. Phys. Plasmas **12** (2005) 122505.
[33]. Smith, H., et al. Phys. Plasmas **13** (2006) 102502.
[34]. Tamai, H., et al., Nucl. Fusion **42** (2002) 290.
[35]. Yoshino, R., et al., Nucl. Fusion **39** (1999) 151.
[36]. Yoshino R. and Tokuda S., Nucl. Fusion **40** (2000) 1293.
[37]. Wesson, J.A., et al., Nucl. Fusion **29** (1989) 641.

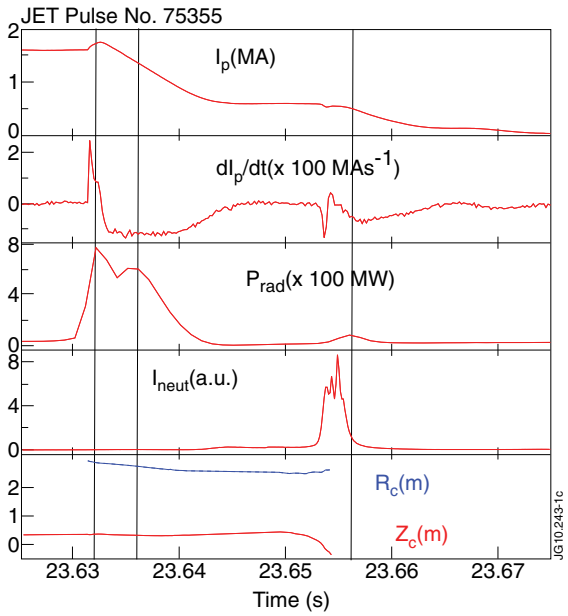

Figure 1. Evolution of the plasma current (I_p), its time derivative dI_p/dt, plasma radiation (P_{rad}) photoneutron emission (I_{neut}) and radial (R_c) and vertical (Z_c) position of the plasma current centroid during a runaway plateau plasma at JET and its termination. The vertical lines correspond to the times for which bolometric reconstructions of the plasma radiation are shown in Fig.2.

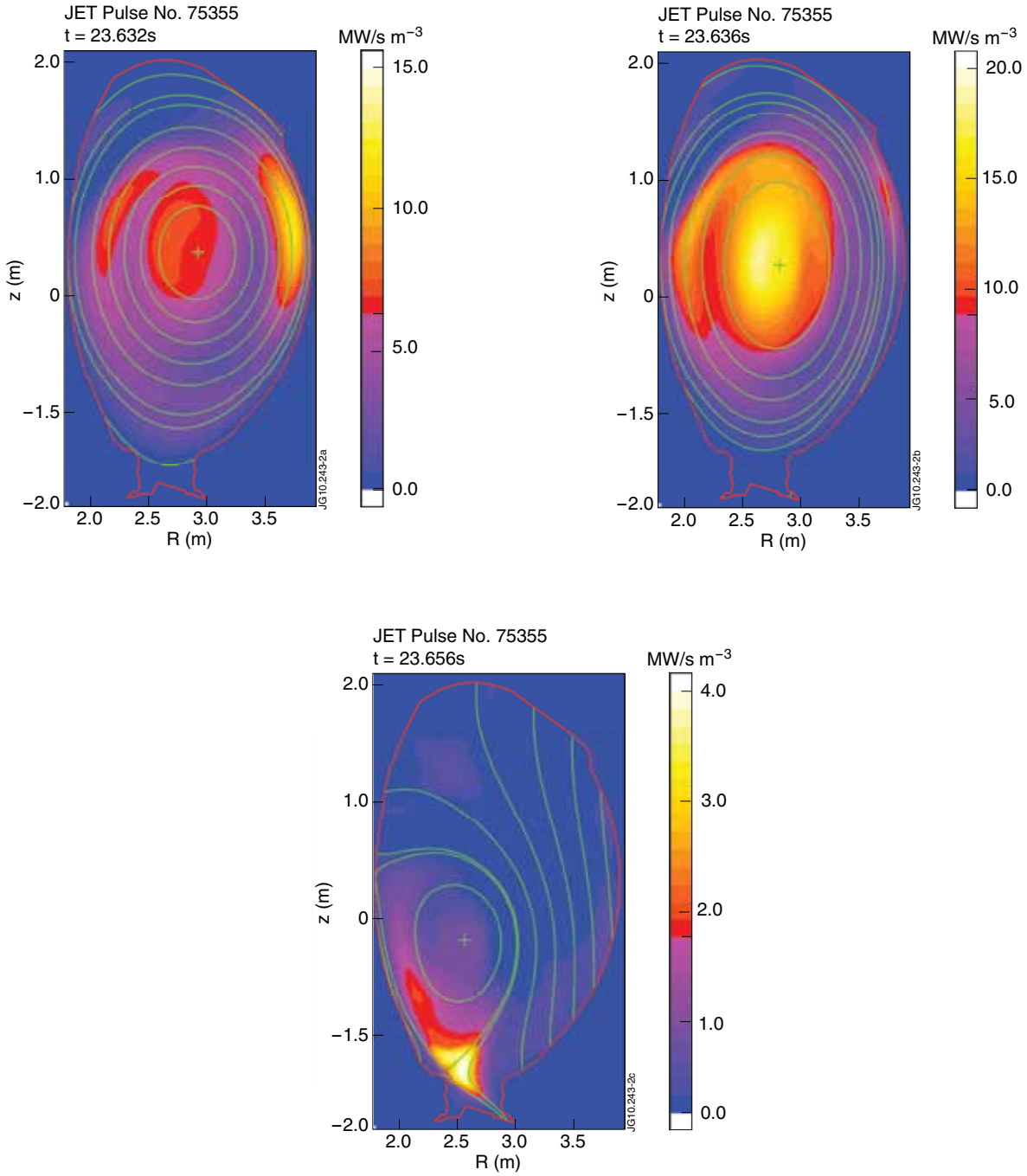

Figure 2. Bolometric reconstructions during : (a) the thermal quench, (b) initial current quench and (c) runaway termination together with the plasma equilibria calculated at the corresponding times. For the last time slide it has not been possible to obtain a converged equilibrium reconstruction at the time of the final radiation peak and the last converged equilibrium reconstruction (at 23.654s, i.e. 2ms before the radiation peak) has been used for the tomographic reconstruction. This is not expected to introduce qualitative differences to the reconstructions (i.e. the localisation of the radiation at the lower region of the vacuum vessel) with respect to the results obtained by using the equilibrium reconstruction at the time of the radiation peak if it were available.

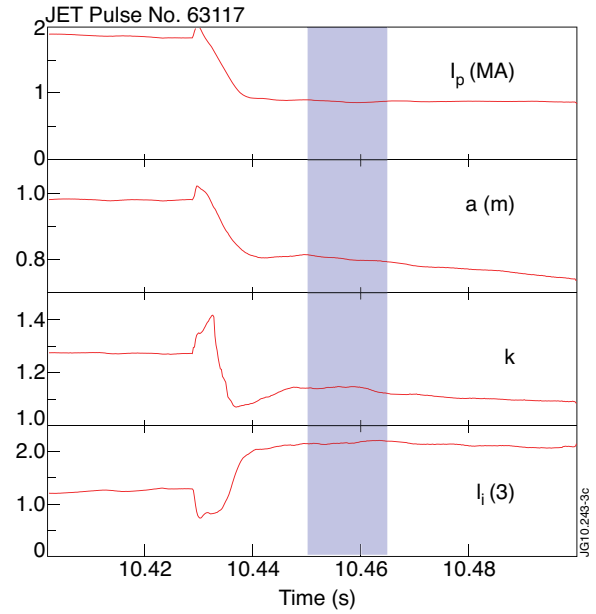

Figure 3. Evolution of the plasma current (I_p), plasma minor radius (a), plasma elongation (κ) and internal inductance (li(3)) during the formation of a runaway plateau plasma at JET. The shaded area corresponds to the time interval for the soft X-ray emission measurements shown in Fig.5.

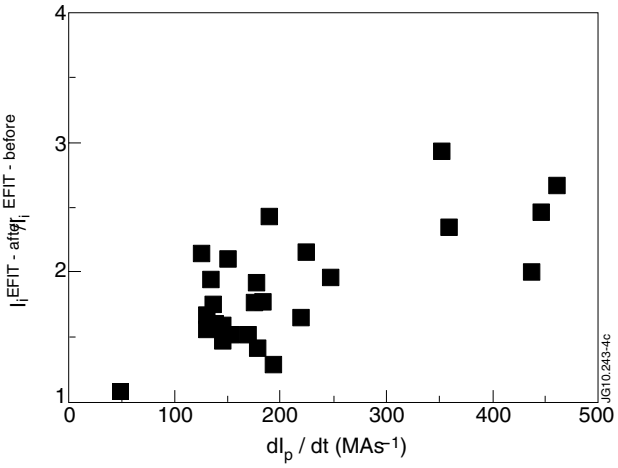

Figure 4. Ratio of the internal inductance of runaway plateau plasmas to that of the pre-disruptive plasma conditions versus initial plasma current derivative in the current quench showing the trend for this ratio to increase with larger plasma current derivatives.

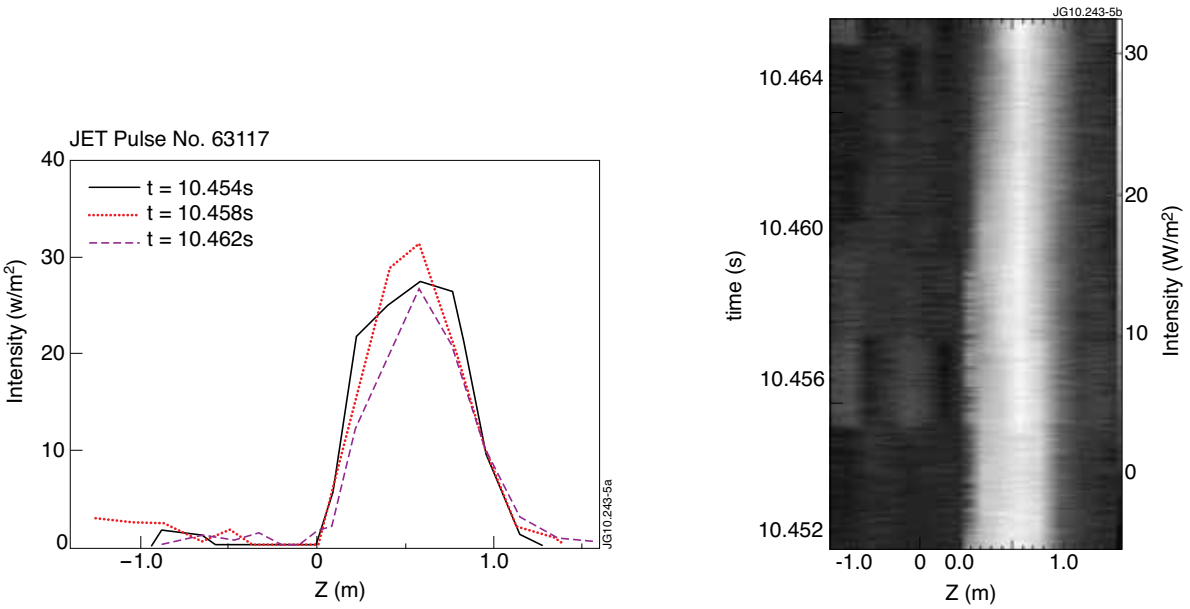

Figure 5. Integrated soft X-ray emission from runaway electrons during the plateau of JET dPulse No: 63117 (Fig. 3) versus the vertical coordinate z (zero corresponds to the midplane of the JET vacuum vessel).

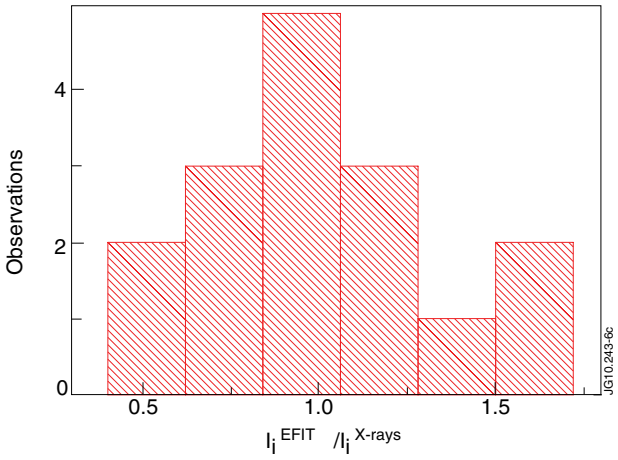

Figure 6. Histogram of the ratio of the plasma internal inductances for runaway plateau plasmas in JET as determined by equilibrium magnetic reconstruction and from the soft X-ray emission profiles by the method described in the text.

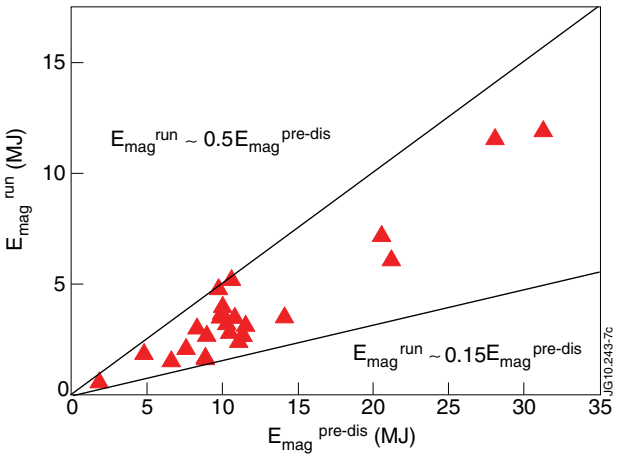

Figure 7. Total magnetic energy of runaway plateau plasmas at JET versus pre-disruptive magnetic plasma energy in these experiments.

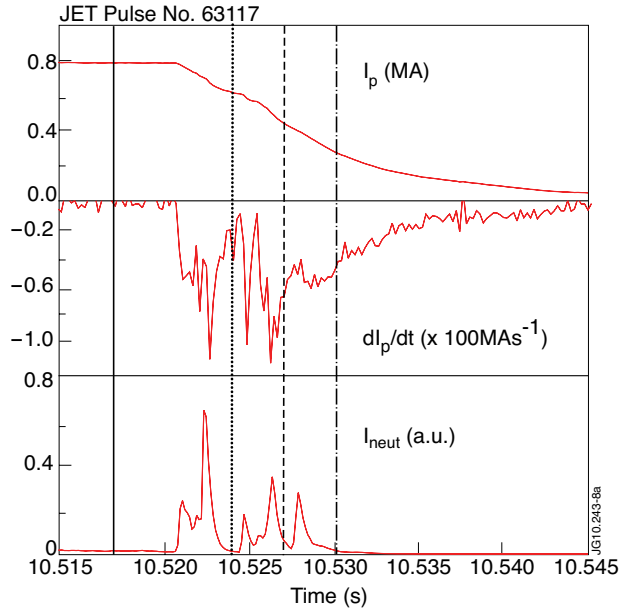

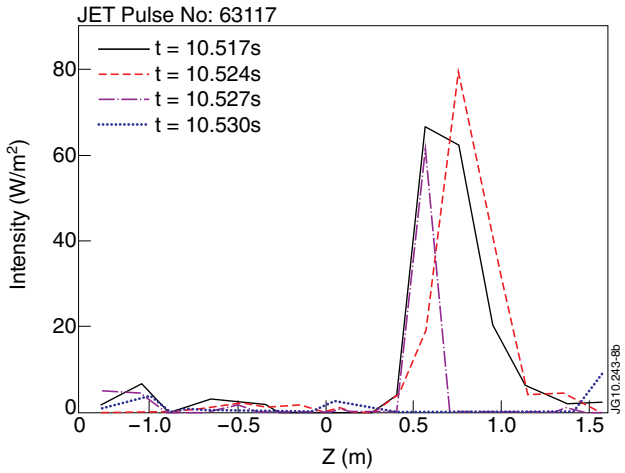

Figure 8. (a) Evolution of the plasma current (I_p), its time derivative dI_p/dt and photoneutron (emission) during the termination of a runaway plateau plasma at JET with multiple runaway electron loss events. The vertical lines correspond to the times for which the soft x-ray emission from runaway electrons are shown in Fig.8b. (b) Integrated soft x-ray emission from runaway electrons during the termination of a runaway plateau discharge with multiple runaway electron loss events versus the vertical coordinate z (zero corresponds to the midplane of the JET vacuum vessel).

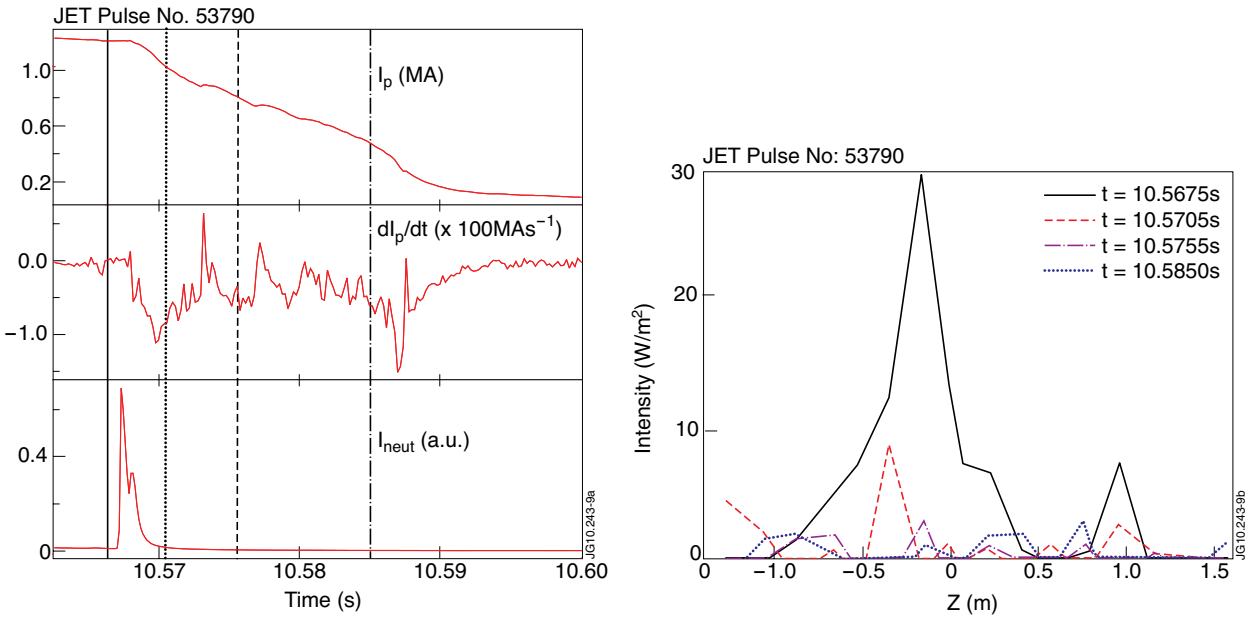

Figure 9. (a) Evolution of the plasma current (I_p), its time derivative dI_p/dt and photoneutron (emission) during the termination of a runaway plateau plasma at JET in with a single runaway electron loss event. The vertical lines correspond to the times for which the soft x-ray emission from runaway electrons are shown in Fig.9b. (b) Integrated soft x-ray emission from runaway electrons during the termination of a runaway plateau discharge with a single runaway electron loss event versus the vertical coordinate z (zero corresponds to the midplane of the JET vacuum vessel).

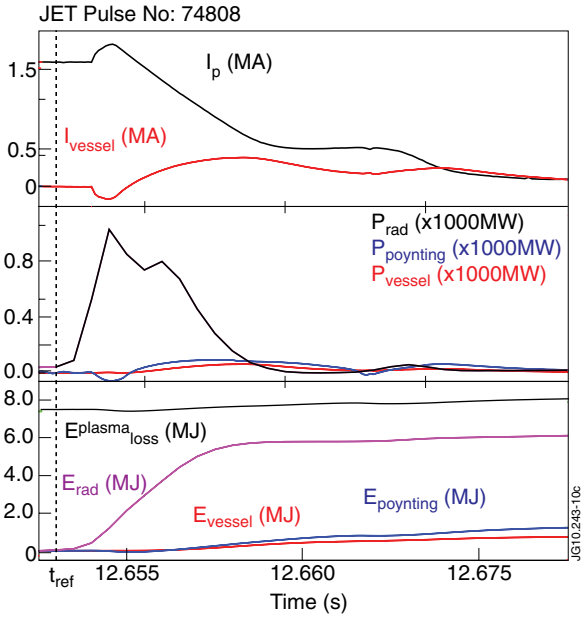

Figure 10. Evolution of the plasma current (I_p), current induced in the vacuum vessel (I_{vessel}), radiated power (P_{rad}), power associated with the influx of magnetic energy into the vessel ($P_{Poynting}$) power dissipated by ohmic heating of the vessel (P_{vessel}) and the corresponding energies (E_{rad}, $E_{Poynting}$ E_{vessel}) for a JET discharge with runaway plateau formation and termination. E^{plasma}_{loss} is the magnetic energy that is available for dissipation by the plasma calculated on the basis of the magnetic energy inside the vacuum vessel at t_{ref} = 12.651s (marked by the dashed vertical line) and Eq. 4.

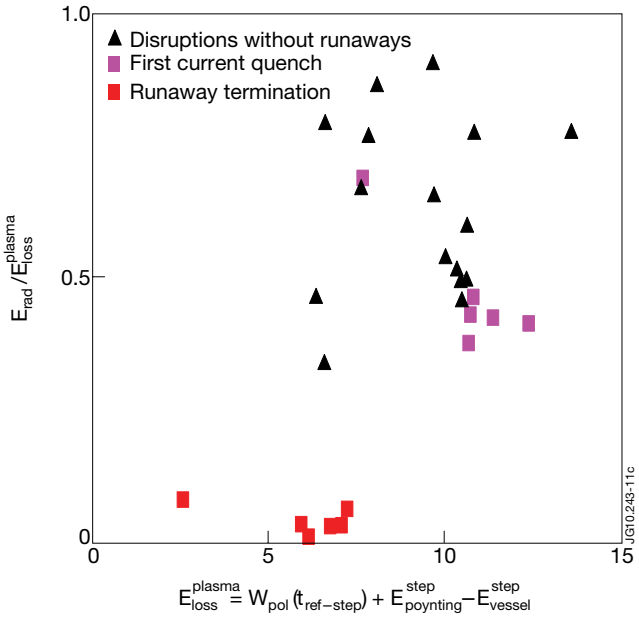

Figure 11. Ratio of the radiated power to the in-vessel magnetic energy available for dissipation by the plasma (E^{plasma}_{loss}) versus in-vessel magnetic energy available for dissipation by the plasma from the analysis in Eq. 4 for the current quench of runaway free disruptions and with runaway plateaus. In the second case the ratio is given for both the initial current quench and for the runaway termination phase.

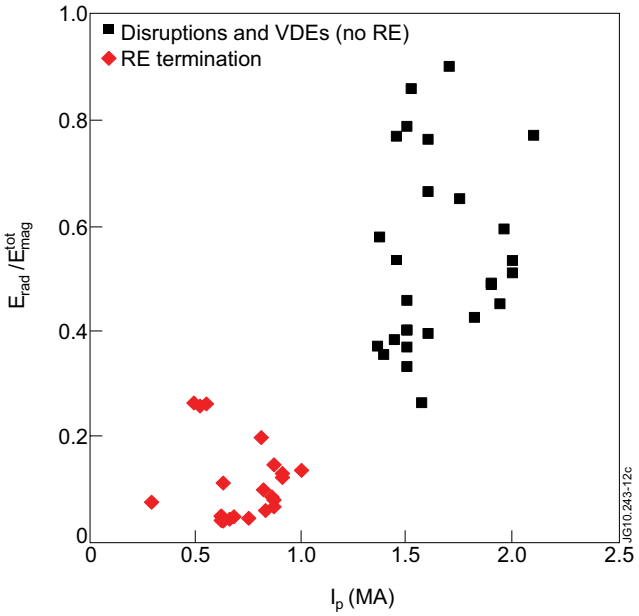

Figure 12. Ratio of the radiated power to the total plasma magnetic energy for the current quench of runaway free disruptions and for the termination of runaway plateaus.

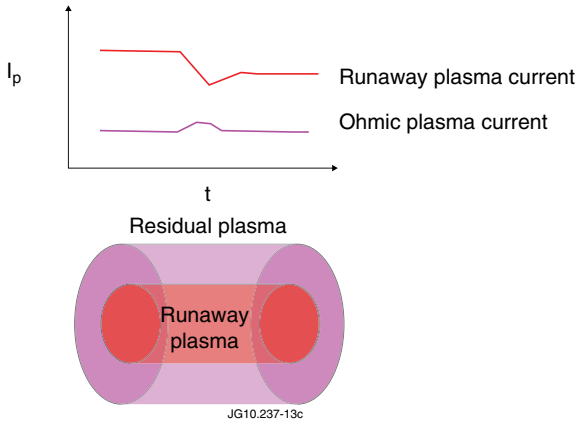

Figure 13. Schematic representation of the expected evolution of the plasma current in the runaway component of a runaway plateau discharge and in the thermal plasma formed after the thermal quench which surrounds the runaway electron plasma.

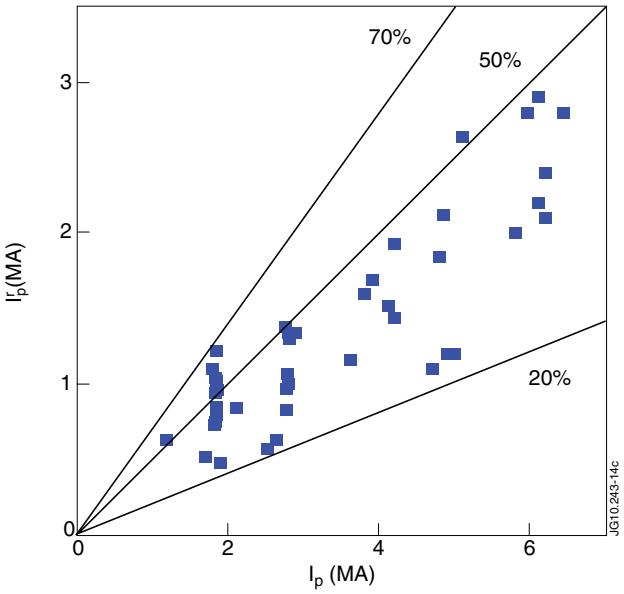

Figure 14. Runaway plateau plasma current (I_p^r) versus pre-disruptive plasma current (I_p) for the discharges utilized for the characterisation of the runaway plateau termination. The lines indicate several ratios of I_p^r/I_p in (%).

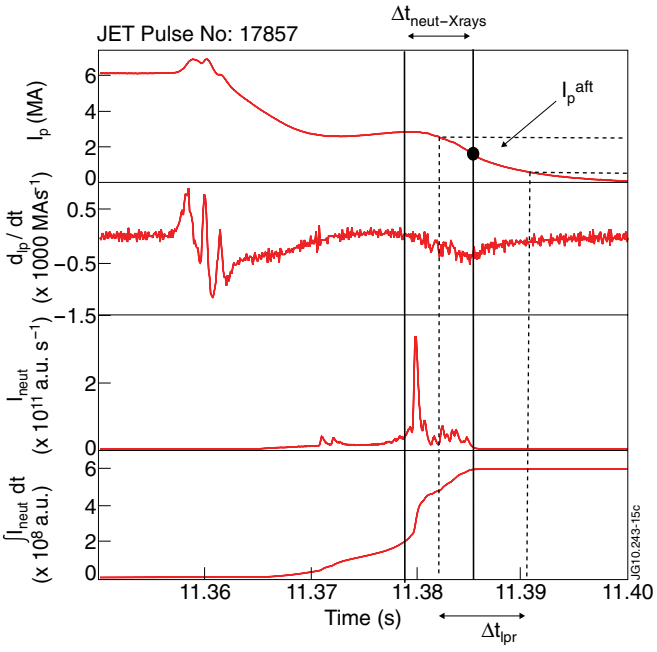

Figure 15. Evolution of the plasma current (I_p), its time derivative dI_p/dt, photoneutron emission (I_{neut}) and integral of the photoneutron emission ($\int I_{neut}\,dt$) during a disruption leading to a runaway plateau plasma at JET and its termination. The vertical lines correspond to the time intervals utilized for the definition of the various timescales described in the text.

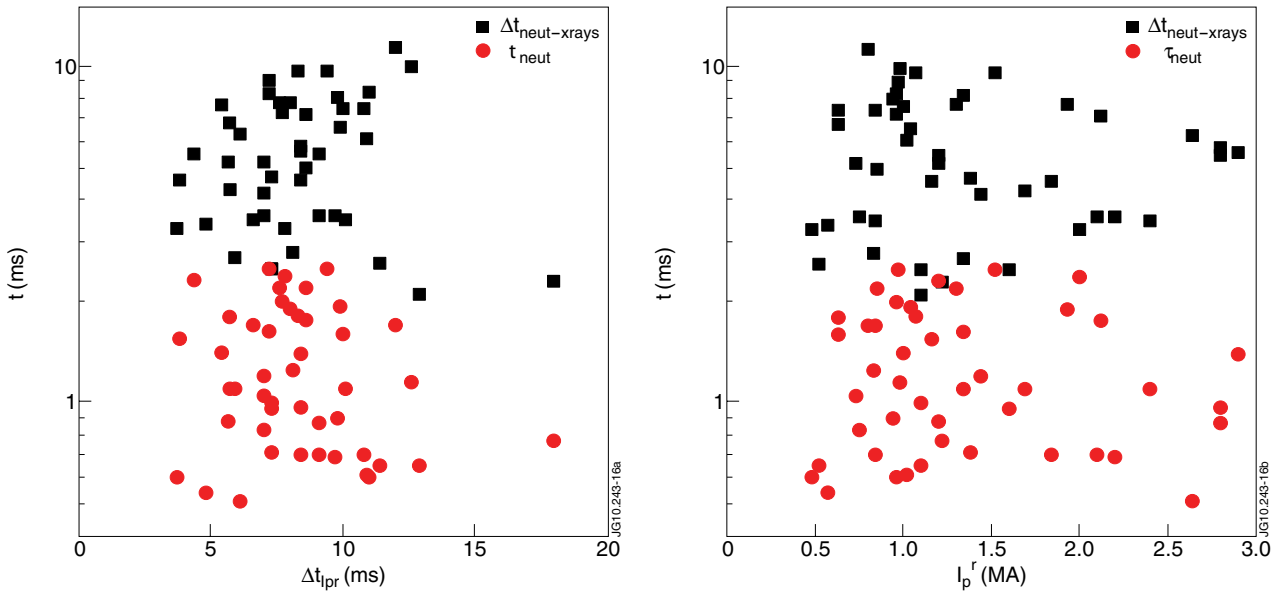

Figure 16. a) Time interval for runaway electron loss ($\Delta t_{neut\text{-}Xrays}$) and timescale for runaway electron loss (τ_{neut}) versus the timescale for plasma current decay during runaway plateau termination phase (Δt_{Ipr}). b) Time interval for runaway loss ($\Delta t_{neut\text{-}Xrays}$) and timescale for runaway electron loss (τ_{neut}) versus runaway plateau plasma current (I_p^r).

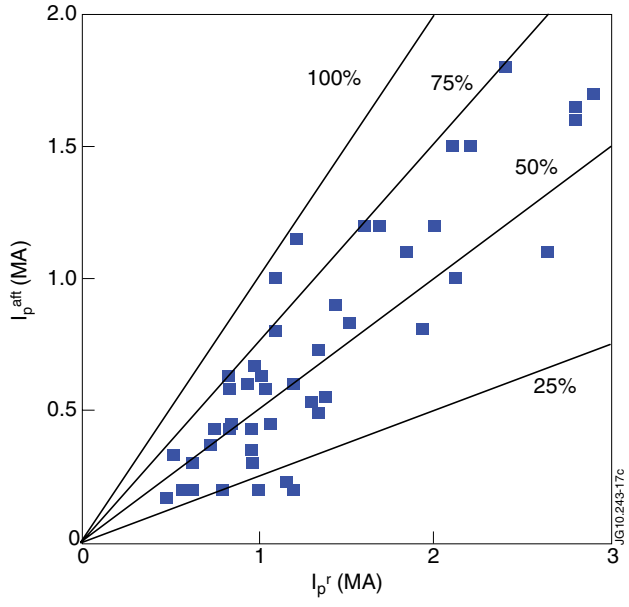

Figure 17. Post-runaway plasma current (I_p^{aft}) versus runaway plateau plasma current (I_p^r) for the dataset analyzed.

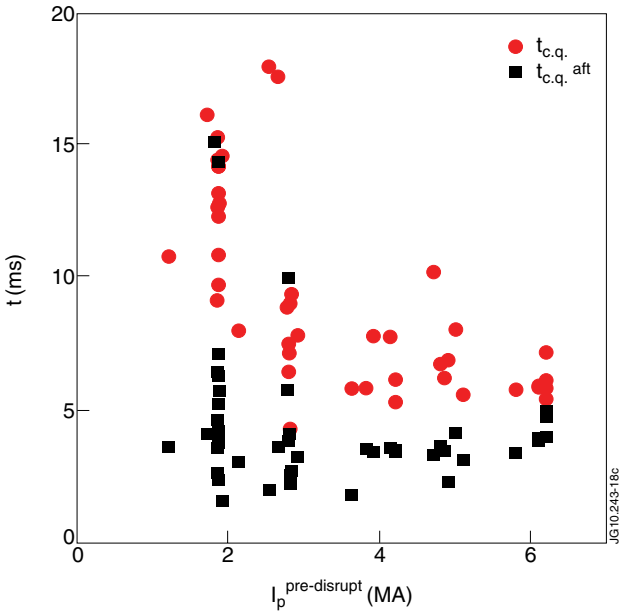

Figure 18. Timescale for the current decay of the initial current quench in discharges with runaway formation ($t_{t.c.}$) and in the post-runaway plasma ($t_{t.c.}^{aft}$) versus pre-disruptive plasma current.

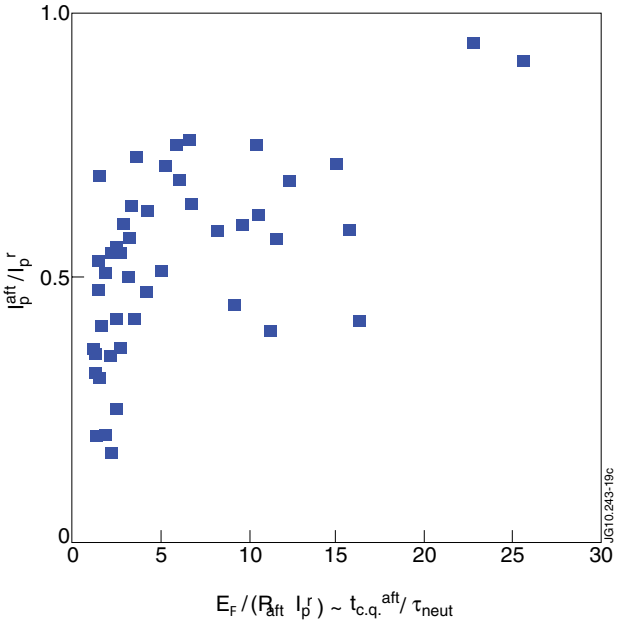

Figure 19. Ratio of the post-runaway plasma current (I_p^{aft}) to the runaway plateau plasma current (I_p^r) versus normalised electric field ($E_\phi/(R_{aft}\ I_p^r)$) as approximated by $t_{c.q.}^{aft}/\tau_{neut}$ showing the more efficient conversion of runway current into ohmic current in the thermal plasma with increasing values of the normalised electric field.

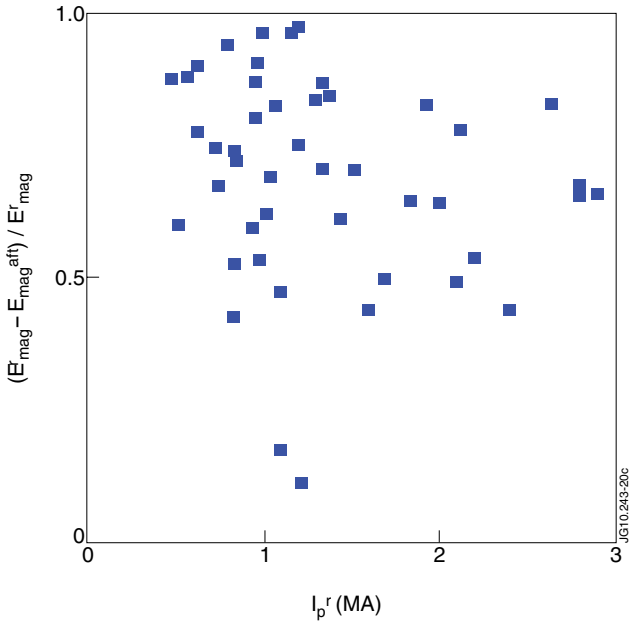

Figure 20. Normalised magnetic energy loss during the runaway loss phase ($\Delta_{tneut\text{-}Xrays}$) to the initial magnetic energy of the runaway plateau plasma versus runaway plasma current (I_p^r). For most of the discharges at JET a significant fraction of the initial magnetic energy of the runaway plateau plasma is lost during this phase.

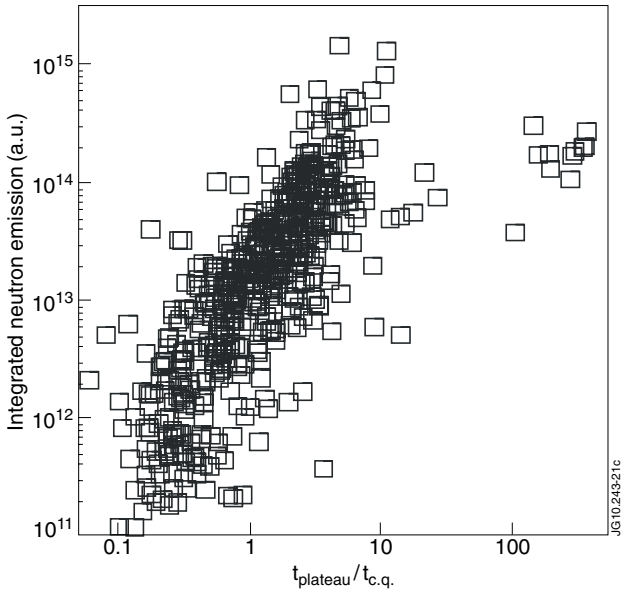

Figure 21. Integrated neutron emission (proportional to the kinetic energy deposited by runaways onto in-vessel components) during the runaway plateau phase of discharges at JET versus the ratio of the plateau duration ($t_{plateau}$) to initial current quench timescale ($t_{c.q.}$). The increase of the integrated neutron emission for $t_{plateau}/t_{c.q.} > 1$ is consistent with the existence of a mechanism (such as conversion of runaway plateau magnetic energy into runway kinetic energy) to increase the runaway electrons kinetic energy beyond that acquired in the initial current quench in the disruption.

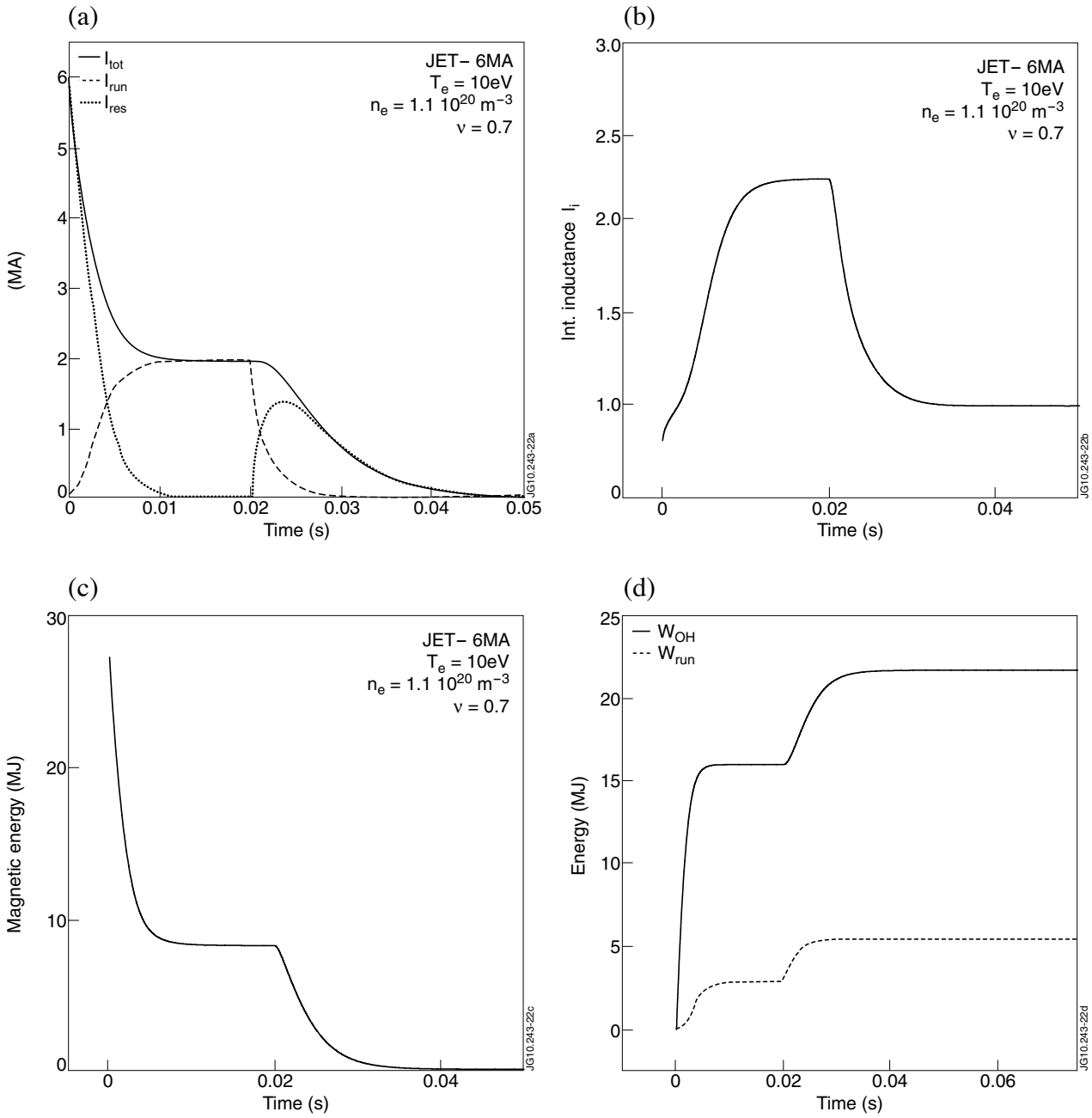

Figure 22. Simulation of a JET disruption with runaway plateau plasma formation and termination: a) Total plasma current (I_{tot}) and its components carried by runaway electrons (I_{run}) and in the thermal plasma (I_{res}) versus time from the disruption thermal quench; b) Evolution of the plasma internal inductance showing a strong peaking during the runaway plateau formation and a decrease during its termination; c) Evolution of the plasma energy magnetic energy; d) Evolution of the plasma magnetic energy dissipated ohmically by the thermal plasma (W_Ω) and converted into runaway electron kinetic energy (W_{run}) during the initial current quench and the termination of the runaway plateau plasma.

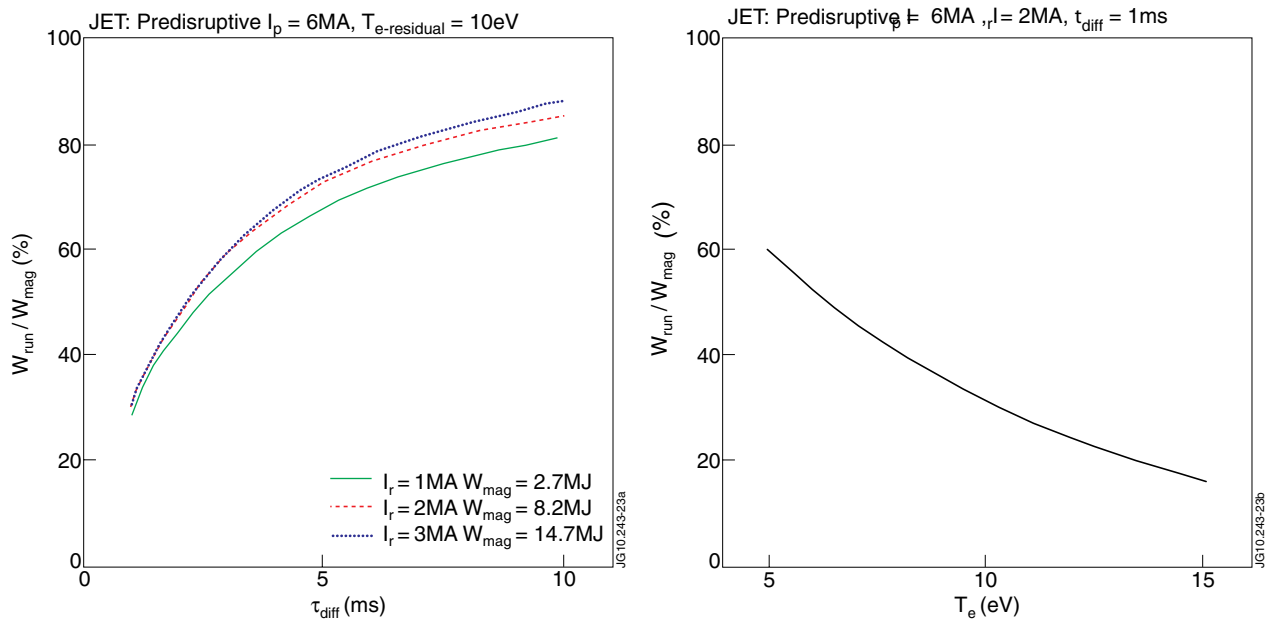

Figure 23. a) Proportion of runaway plateau magnetic energy (W_{mag}) converted into runaway electron kinetic energy (W_{run}) versus the timescale for runaway loss (τ_{diff}) and various levels of runaway plateau current at JET. b) Proportion of runaway plateau magnetic energy converted into runaway electron kinetic energy versus temperature in the thermal plasma for a runaway plateau current of 2 MA at JET (τ_{diff} = 1ms).

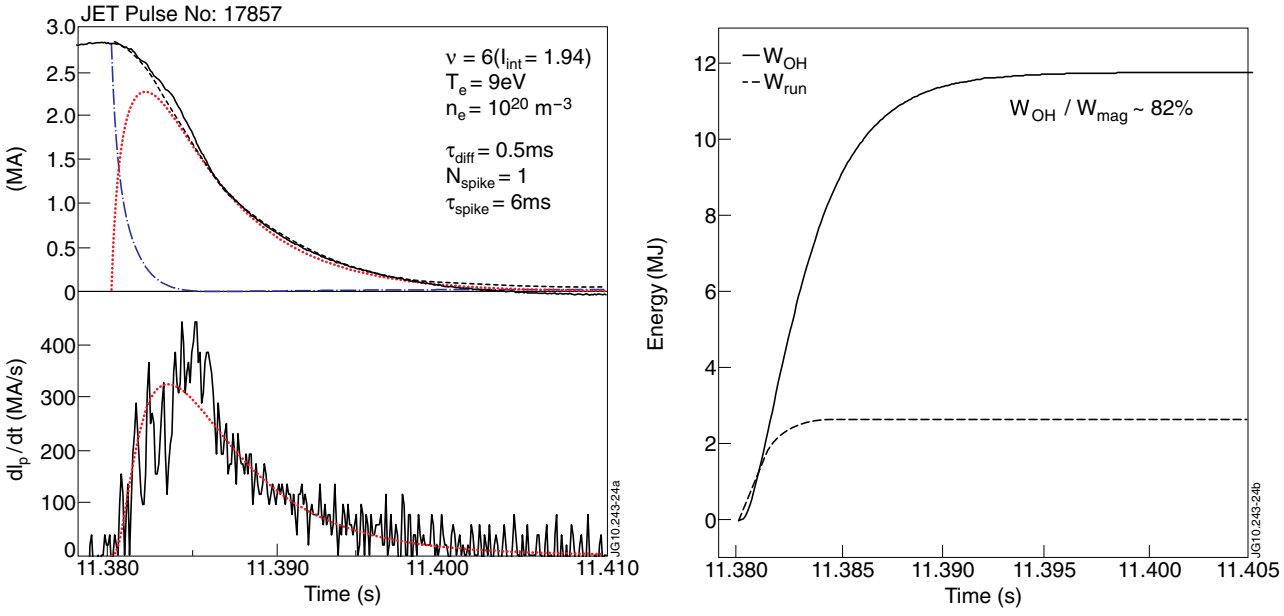

Figure 24. Simulation of the termination of a JET runaway plateau in which runaways are predominantly lost in a single event, from hard X-ray and photoneutron measurements. a) Top. Total plasma current (in black) and its components carried by runaway electrons (blue) and in the thermal plasma (red). Bottom measured total plasma current derivative (in absolute value) during the runaway plateau termination phase (black) and simulated results from the calculations in the top figure (red); b) Evolution of the plasma magnetic energy dissipated ohmically by the thermal plasma (W_{OH}) and converted into runaway electron kinetic energy (W_{run}) during the termination of the runaway plateau plasma.

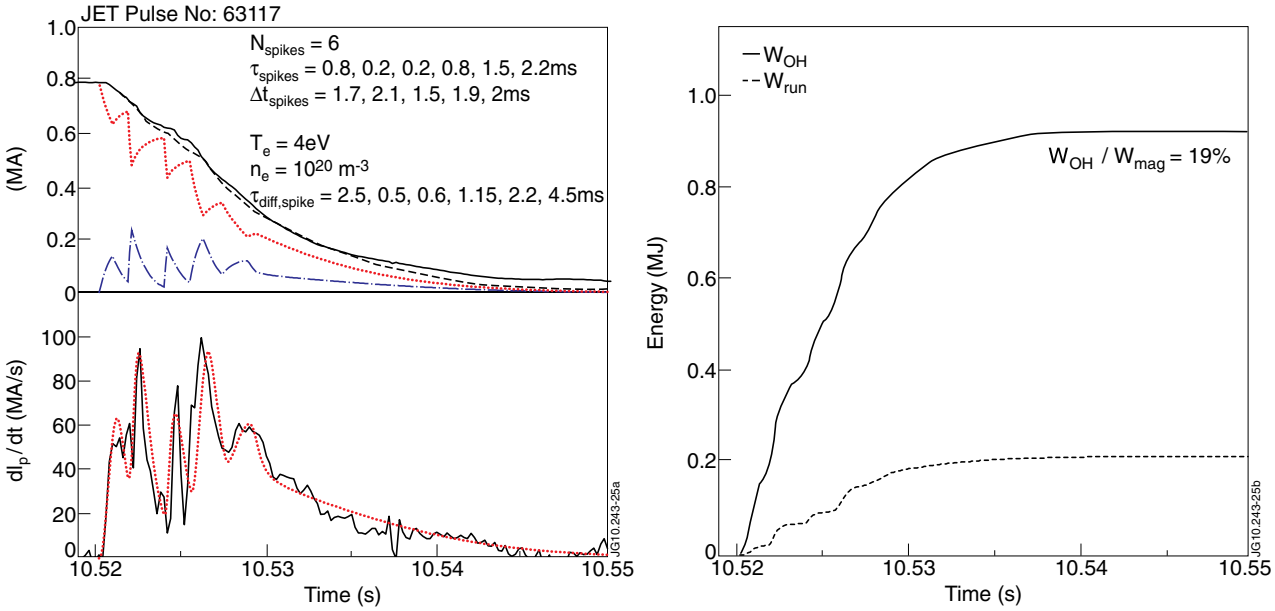

Figure 25. Simulation of the termination of a JET runaway plateau in which runaways are lost in a series of events over an extended period, from hard X-ray and photoneutron measurements. a) Top. Total plasma current (in black) and its components carried by runaway electrons (red) and in the thermal plasma (blue). Bottom measured total plasma current derivative (in absolute value) during the runaway plateau termination phase (black) and simulated results from the calculations in the Top figure (red); b) Evolution of the plasma magnetic energy dissipated ohmically by the thermal plasma (W_{OH}) and converted into runaway electron kinetic energy (W_{run}) during the termination of the runaway plateau plasma.

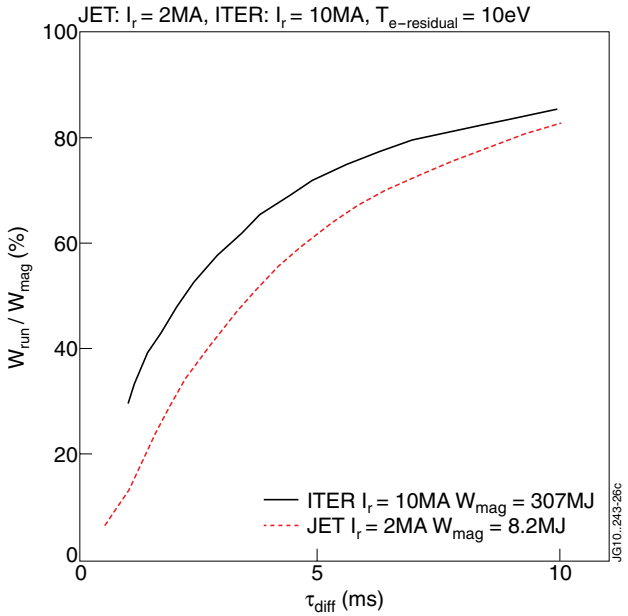

Figure 26. Proportion of runaway plateau magnetic energy converted into runaway electron kinetic energy versus the timescale for runaway loss (τ_{diff}) for ITER (I_r = 10 MA) and JET (I_r = 2 MA).